

**MODELING BICOMPONENT ADSORPTION OF AROMATIC COMPOUNDS  
ONTO NONPOLAR POLYMERIC RESIN MN200**

---

A Thesis  
Submitted to  
the Temple University Graduate Board

---

In Partial Fulfillment  
of the Requirements for the Degree  
MASTER OF SCIENCE  
IN ENVIRONMENTAL ENGINEERING

---

by  
Shubo Wang  
July 2015

Thesis Approvals:

Dr. Huichun (Judy) Zhang, Thesis Advisory Committee Chair, Civil and Environmental  
Engineering, Temple University  
Dr. Benoit Van Aken, Civil and Environmental Engineering, Temple University  
Dr. Rominder Suri, Civil and Environmental Engineering, Temple University

## ABSTRACT

A large number of organic contaminants are commonly found in industrial and municipal wastewaters. Aromatic compounds, such as phenol, aniline and their derivatives, are contaminants of high priority and usually coexist in waste streams from industries of, for example, aromatic amine compounds and ammonolysis of phenols. Thus, for proper unit design to remove contaminant mixtures by adsorption, multi-component adsorption models are necessary. The present work was aimed at examining the applicability of Ideal Adsorbed Solution Theory (IAST), a prevailing thermodynamic model, and its derivative i.e. Segregated IAST (SIASST) and Real Adsorbed Solution Theory (RAST) to multi-solute adsorption from the aqueous phase, specifically, bi-solute adsorption of phenols, anilines and nitrobenzene onto a hyper-crosslinked polystyrene resin, MN200. Based on the experimental bi-solute adsorption isotherms, we have successfully developed methods for modeling with RAST incorporated with Wilson equation, Nonrandom two-liquid (NRTL) model, and an empirical four-parameter equation developed in this work. It turns out that our proposed four-parameter equation can fit the activity coefficients,  $\gamma_i$ , better than the other two equations and thus enhanced the accuracy of RAST in predicting bi-solute adsorption equilibrium. Besides successfully developing methods for properly designing binary-solute batch experiments and accurately modeling with RAST, two empirical linear relationships have been developed for the adsorption of a number of infinite dilute solutes in the presence of a major contaminant (either 4-methylphenol or nitrobenzene). Results show that polyparameter linear free energy relationships have a great potential in predicting adsorbed phase activity coefficients of solutes when the adsorbed amounts are dominated

by the major contaminant and the adsorbed mixture resembles infinite dilute solution. Activity coefficients under such conditions were represented by  $\gamma_i^\infty$  and were successfully extrapolated to  $\gamma_i$  at non-infinite conditions by  $\gamma_i$  models i.e. Wilson equation. To the best of our knowledge, this is the first systematic study predicting adsorbed phase activity coefficients for bi-solute adsorption. In addition, our tri- and tetra-solute adsorption data showed that the predominating solute, NB in this case, solely contributed to the competitive effect while the dilute solutes tend not to interact with each other. This indicates that for each solute, the competitive effects can be independently considered and a multi-component system with  $n$  components but only one component dominating can be treated as  $(n-1)$  bi-solute systems separately. This will significantly simplify the calculation for modeling multi-component adsorption while it is also close to many real systems where there is one major contaminant or a large amount of NOM in present. Our findings have proved a major step forward to accurately modeling multi-solute adsorption for proper unit design of adsorption processes.

## **ACKNOWLEDGEMENTS**

This study has been partly funded by Pennsylvania Water Resources Research Center and Water and Environmental Technology Center of National Science Foundation Industry/University Cooperative Research at Temple University, Philadelphia. Funding is gratefully acknowledged. The author is very thankful for the guidance of research by all thesis examining committee members, Dr. Rominder Suri, Dr. Benoit Van Aken, and especially Dr. Huichun (Judy) Zhang, and also the assistance of lab members including Dr. Bingjun Pan, Nicholas Kheny, Zaid Shah, Ryan Slobodjian, and Paul Senker.

## TABLE OF CONTENT

<b>ABSTRACT</b> .....	<b>ii</b>
<b>ACKNOWLEDGEMENTS</b> .....	<b>iv</b>
<b>LIST OF FIGURES</b> .....	<b>vii</b>
<b>LIST OF TABLES</b> .....	<b>viii</b>
<b>LIST OF ACRONYMS</b> .....	<b>ix</b>
<b>CHAPTER 1 INTRODUCTION</b> .....	<b>1</b>
1.1 Background and Motivation.....	1
1.2 Problem Statement .....	2
1.3 Research Objectives .....	4
<b>CHAPTER 2 LITERATURE REVIEW</b> .....	<b>6</b>
2.1 Adsorbed Solution Theories (ASTs).....	6
2.1.1 Ideal AST and Nonideal ASTs .....	6
2.1.2 AST Basic Thermodynamic Theory.....	9
2.1.3 Effects of Single Solute Adsorption Isotherm Models.....	10
2.1.4 Activity Coefficients of Adsorbates in Adsorbed Mixtures .....	12
2.2 Segregated Adsorption Models .....	12
2.3 Multi-solute Adsorption .....	14
2.4 Polymeric Resin Adsorbent.....	16
<b>CHAPTER 3 EXPERIMENTAL AND MODELING APPROACH</b> .....	<b>17</b>
3.1 Adsorption isotherms .....	17
3.1.1 Solutes and Adsorbent .....	17
3.1.2 Batch Adsorption Experiments.....	18

3.1.3	Error Analysis.....	19
3.1.4	Selection of Single Solute Models.....	19
3.1.5	Solution of IAST .....	22
3.1.6	Multi Solute Dual-Site Langmuir (MSDSL).....	25
3.1.7	Segregated Ideal Adsorbed Solution Theory (SIAST).....	26
3.1.8	Design of Binary Adsorption Experiments .....	28
3.2	Real adsorbed Solution Theory (RAST) and $\gamma_i$ Modeling.....	29
3.2.1	Calculation of $\gamma_i$ Based on Experimental Data .....	29
3.2.2	Fitting Equations for Adsorbed Phase Activity Coefficients .....	34
3.3	Polyparameter Linear Free Energy Relationship (pp-LFER) .....	38
<b>CHAPTER 4 RESULTS AND DISCUSSION.....</b>		<b>41</b>
4.1	Single-Solute Adsorption.....	41
4.2	Modeling Binary-Solute Adsorption.....	43
4.2.1	Comparison of IAST with SIAST and MSDSL.....	43
4.2.2	Comparison of RAST Incorporated with Wilson Equation, NRTL Model, and FPM	46
4.3	Adsorbate-Adsorbate Interactions and pp-LFER.....	56
4.4	Tri- and Tetra-Solute Adsorption of Aniline, Phenol, and 4-MP in the Presence of a High Concentration of Nitrobenzene .....	62
<b>CHAPTER 5 CONCLUSIONS.....</b>		<b>65</b>
<b>CHAPTER 6 FUTURE WORK .....</b>		<b>67</b>
<b>REFERENCES CITED .....</b>		<b>68</b>

## LIST OF FIGURES

<b>Figure 1.</b> Experimental data of single solute adsorption of 8 aromatic compounds onto MN200. Adapted from ref <sup>69</sup> .....	20
<b>Figure 2.</b> Two proposed integration paths for eq. 54.....	31
<b>Figure 3.</b> Procedure for iterative calculation of RAST with $\gamma_i$ calculated based on fitting equations.....	37
<b>Figure 4.</b> Calculated reduced spreading pressures of 8 aromatic compounds as single solutes as a function of equilibrium concentration.....	42
<b>Figure 5.</b> Binary adsorption of 4-MP (the primary solute) and aniline (the competitor). 46	
<b>Figure 6.</b> Plots of binary adsorption data in <b>Table 6</b> and prediction results by IAST and RAST- $\gamma_i^{exp}$ .....	50
<b>Figure 7.</b> Experimental activity coefficients fitted by Wilson, NRTL and FPM equations. ....	51
<b>Figure 8.</b> Comparison of experimental data of the test sets with prediction by RAST- Wilson, RAST-NRTL, RAST-FPM, and IAST .....	55
<b>Figure 9.</b> Compare calculated $\gamma_i^\infty$ based on linear relationships with $\gamma_i^\infty$ obtained experimentally. The dashed lines represent 10% errors of $\gamma_i^\infty$ prediction which will result in about 9~11% error in the predicted adsorbed amount according to Eq. 73	60
<b>Figure 10.</b> Prediction errors of the adsorbed amounts of aniline in the presence of 4-MP (test set) using $\gamma_i$ extrapolated from $\gamma_i^\infty$ .....	61
<b>Figure 11.</b> Tri- and tetra-solute adsorption of aniline, phenol, and 4-MP in the presence of a high concentration of nitrobenzene ~ 0.45 mM. ....	64

## LIST OF TABLES

<b>Table 1.</b> Equations of the common single-solute isotherm models.....	11
<b>Table 2.</b> Physical-chemical properties of selected aromatic compounds.....	17
<b>Table 3.</b> Fitting results of single-solute isotherm models .....	21
<b>Table 4</b> Binary adsorption equilibrium data with 4-MP as the primary solute and aniline as the competitor and model prediction based on IAST, SIAST, and MSDSL. ....	44
<b>Table 5.</b> Summary of prediction results of IAST, SIAST and DSL.....	46
<b>Table 6.</b> Fitting results of the isotherms of primary solutes in binary mixtures and prediction results of $q_e$ by RAST- $\gamma_i^{exp}$ .....	49
<b>Table 7.</b> Fitting results of $\gamma_i$ by NRTL model, Wilson equation, and FPM.....	54
<b>Table 8.</b> Prediction of the test sets by RAST with NRTL model, Wilson equation, and FPM.....	54
<b>Table 9.</b> Infinite dilution activity coefficients calculated from NRTL model, Wilson equation, and FPM by letting $z_i$ be zero for each solute .....	56
<b>Table 10.</b> Infinite dilution activity coefficients calculated based on FPM as shown in <b>Table 9</b> and solute Abraham descriptors .....	58

## LIST OF ACRONYMS

4-CA	4-chloroaniline
4-CP	4-chlorophenol
4-MP	4-methylphenol
4-NA	4-nitroaniline
4-NP	4-nitrophenol
AST	Adsorbed solution theory
D-A	Dubinin-Astakhov ( model)
DI	De-Ionized
DSL	Dual-site Langmuir (model)
EBC	Equivalent background compound
FPM	Four-parameter model
HIAST	Heterogeneous ideal adsorbed solution theory
HPLC	High-performance liquid chromatography
IAST	Ideal adsorbed solution theory
LSE	Least square error
MN200	PUROLITE MACRONET MN-200 resin
MSDSL	Multi-solute dual-site Langmuir (model)
MWSE	Mean weighted square error
NB	Nitrobenzene
NIAST	Nonideal adsorbed solution theory

NOM	Natural organic matter
NRTL	Nonrandom two-liquid (model)
OC	Organic contaminant
PRAST	Predictive real adsorbed solution theory
RAST	Real adsorbed solution theory
RE	Relative error
RMSE	Root mean square error
SIAST	Segregated ideal adsorbed solution theory
SPD	Spreading pressure dependent (model)
UNIQUAC	UNIversal QUAsiChemical
$C_e$	Equilibrium concentration in aqueous phase
$q_e$	Adsorbed amount in adsorbed phase
$\Psi$	Reduced spreading pressure
$\gamma_i$	Adsorbed phase activity coefficient
$\gamma_i^{exp}$	Calculated adsorbed phase activity coefficient based on experimental data
$\pi$	Spreading pressure, surface tension, surface potential, or grand potential in literatures
$mM$	mmol/L

# CHAPTER 1

## INTRODUCTION

### 1.1 Background and Motivation

The occurrence of a large number of organic contaminants (OCs) in our water systems and in the environment is among the greatest environmental challenges facing the world. Examples include priority contaminants such as pesticides, dyestuffs, petrochemicals, and chemical intermediates, and emerging contaminants such as pharmaceutical and personal care products. Their broad range of applications and relatively inefficient removal from waste streams have led to their ubiquitous presence in drinking water, wastewater and many environments, including surface water, groundwater, soils and sediments.<sup>1-4</sup> The persistence of OCs in the aquatic environment likely poses serious threats to ecosystems and human health. Adsorption is one of the most frequently used methods for the removal of OCs from contaminated water.<sup>5-7</sup> During the application of a given adsorbent, adsorption equilibrium data over a broad range of solute concentrations are among the most important limits, they can also affect the overall cost of the treatment system.<sup>8</sup>

Contaminated waters typically contain mixtures of OCs while the presence of a single-solute is likely the exception rather than the rule, so proper design of an efficient adsorption system requires reliable adsorption equilibrium data of the multi-solute mixture, i.e. the adsorbed amount of each adsorbate and the composition of the solution phase at equilibrium (adsorption isotherms). However, it is time-consuming and difficult to experimentally obtain all the equilibrium data for the vast number of OC mixtures. As

a result, most adsorption studies limit their efforts to studying adsorption of single solutes. Predictive models that can be used to accurately predict equilibrium data for multi-component adsorption based on the available single solute adsorption isotherms will be extremely valuable.

## 1.2 Problem Statement

For the purpose of applying adsorption processes to the removal of several contaminants simultaneously from contaminated water, competitive effects in multi-solute systems have to be thoroughly considered because of the fact that they can decrease adsorption capacity compared to that of single-solute adsorption systems. Thus, accurate data of multi-solute adsorption equilibrium is desirable for either batch adsorption or dynamic column adsorption.<sup>9</sup> Since mathematical modeling is more time-saving and economically acceptable than experimental methods in determining adsorption capacity,<sup>10</sup> the goal of this work was to improve the efficiency of modeling for multi-solute adsorption equilibrium.

Ideal adsorbed solution theory (IAST)<sup>11,12</sup> is among the most prevailing thermodynamic multi-component adsorption models for adsorption from both the gas phase and the aqueous phase. Since ideal behavior, an intrinsic assumption of IAST, is seldom encountered in real systems, a number of modifications of IAST have been derived for gas mixtures, for instances, real adsorbed solution theory (RAST),<sup>13</sup> spreading pressure dependent (SPD) model,<sup>14</sup> predictive real adsorbed solution theory (PRAST),<sup>15</sup> and nonideal adsorbed solution theory (NIAST).<sup>16</sup> The deviation of IAST prediction from experimental data, mainly due to nonideality of adsorbed mixtures, has been attributed by

some researchers to the energetic heterogeneity of adsorption sites and thus, heterogeneous IAST (HIAST),<sup>17</sup> segregated IAST (SIAST)<sup>18</sup> and dual-site Langmuir models have been developed.<sup>19, 20</sup>

Despite the above mentioned achievements in multicomponent adsorption for gas mixtures, little progress has been made in modeling multi-solute adsorption from the aqueous phase. Therefore, it is worthy of extending the recent approaches of modeling gas phase adsorption to multi-solute adsorption. However, for aqueous phase adsorption, it is unclear whether the same assumptions can be acceptable.<sup>8, 21, 22</sup> For example, solvent effects are a driving force in aqueous phase adsorption but not in the gas phase. Hydrophobic effects in water contribute to 60%~85% of Gibbs free energy of adsorption depending on the adsorbent.<sup>23</sup> Since heterogeneity of adsorption energy is a adsorbent related property and is associated with adsorbent-adsorbate interactions, it is reasonable to question, in aqueous phase adsorption systems where adsorbent-adsorbate interactions are not the only driving force of adsorption, whether intermolecular interactions between different adsorbates can also be neglected as in gas-phase adsorption. Thus, the influence of adsorbate-adsorbate interactions on the nonideality of adsorbed mixtures was also investigated in this work in addition to mathematical modeling.

Most studies of multi-solute adsorption were conducted on binary adsorption of only two or three compounds.<sup>8, 21, 22, 24-28</sup> This is mainly due to the intensive labors required to collect multi-component adsorption data. A comparison of competitive adsorption among a diverse range of solutes can provide more information about the competition mechanism, which can in turn lead to the development of more

representative multi-component adsorption models. So far, there has not been a rigorous discussion on the mechanism of nonideality in multi-solute adsorption equilibrium.

In summary, it is desirable to examine the validity of gas phase adsorption models and apply them to aqueous phase adsorption with necessary modification. For this purpose, binary adsorption experiments of a larger number of compounds with diverse physical-chemical properties were conducted to help understand the mechanisms of competitive adsorption and to develop accurate prediction models.

### 1.3 Research Objectives

- i. To use IAST to compare the ability of all solutes to compete for adsorption sites based on their single solute adsorption isotherms. (**Section 4.1**)
- ii. To experimentally obtain binary adsorption isotherms of 8 aromatic compounds, phenol, 4-methylphenol, 4-chlorophenol, 4-nitrophenol, aniline, 4-chloroaniline, 4-nitroaniline, and nitrobenzene, under varying solute ratios onto polymeric resin MN200. These aromatic compounds can be involved in diverse molecular interactions, especially H-bonding and  $\pi$ - $\pi$  electron-donor-acceptor (EDA) interactions.
- iii. To apply IAST, RAST, SIAST and multi-solute dual-site Langmuir (MSDSL) to predicting adsorption equilibrium of bi-solute systems. RAST was incorporated with adsorbed phase activity coefficients to eliminate the deviation of IAST. SIAST and MSDSL assume heterogeneous adsorption sites and were studied for comparison. (**Sec 4.2.1**)

- iv. To calculate adsorbed phase activity coefficients of each solute in all the studied mixtures and model them with classical equilibrium models for liquid mixtures including Wilson, NRTL, and a four parameter empirical equations, developed in this work. This was to test if thermodynamic activity coefficient equations without spreading pressure dependency can be used to fit experimental activity coefficients and whether a better simulation and prediction of multicomponent adsorption equilibrium can be achieved through RAST. (**Section 4.2.2**)
- v. To correlate adsorbed phase activity coefficients of solutes with solutes-molecular descriptors associated with different aromatic substituent groups, namely, amine, hydroxyl, chlorine, methyl and nitro groups. Definition, calculation, and application of adsorbed phase infinite activity coefficients are given in **Sections 3.2.1 and 4.3**.
- vi. To further understand the mechanisms of nonideal competitive adsorption of aromatic compounds on MN200 resin by conducting tri- and tetra-solute adsorption experiments. (**Section 4.4**)

## CHAPTER 2

### LITERATURE REVIEW

#### 2.1 Adsorbed Solution Theories (ASTs)

##### 2.1.1 Ideal AST and Nonideal ASTs

Among existing models to predict multicomponent adsorption, IAST that is based on thermodynamically consistent approaches and relies solely on single-component isotherms has been the most successful.<sup>11, 24, 29-31</sup> IAST was initially developed to predict adsorption equilibrium data of gas mixtures<sup>11</sup> and was later extended to predict adsorption equilibrium of liquid mixtures.<sup>12</sup> IAST has gained a large success in modeling gas-phase adsorption of mixed volatile organic compounds (VOCs).<sup>11, 31, 32</sup> It also has some success in modeling multi-component adsorption from water.<sup>4, 21, 24, 30, 33-38</sup>

Although IAST is not limited to a specific single component isotherm equation, Crittenden et al.'s method of using Freundlich isotherm has been one of the most popular for aqueous phase adsorption due to its explicit analytical expression and better fitting of single solute isotherms. This method was later extended to study the adsorption of contaminants in the presence of natural organic matter (NOM) as an equivalent background compound (EBC).<sup>39-42</sup>

When the adsorbed phase mixture is not ideal and IAST prediction deviates from experimental adsorption equilibrium, a correction of IAST is needed. Although Myers and Prausnitz (1965) incorporated adsorbed phase activity coefficients in IAST in their original work, Costa et al. first extended IAST to Real Adsorbed Solution Theory (RAST) by fitting Gibbs excess free energy models such as Wilson equation and

UNIQUAC to experimental adsorbed phase activity coefficients of binary component adsorption, and then predicted ternary component adsorption with a good accuracy.<sup>13</sup> One favorable feature of Wilson and UNIQUAC models is that only binary parameters are required to predict multi component equilibrium, however, both models only considered the composition dependency of adsorbed phase activity coefficients. Talu and Zwiebel proposed a spreading pressure dependent (SPD) model to correlate adsorbed phase activity coefficient with spreading pressure.<sup>14</sup> However, SPD requires the isosteric heat of adsorption which is obtained from adsorption isotherms at different temperatures and thus requires more experimental work. Another method to account for spreading pressure dependency is to express excess Gibbs free energy as the product of a traditional model like Wilson, Margules, and UNIQUAC and an empirical exponential equation of spreading pressure.<sup>43</sup> Other models that were fitted to adsorbed phase activity coefficients include NRTL,<sup>44</sup> Flory Huggins equation<sup>45</sup> and a two-parameter Margules equation.<sup>46</sup> Furmaniak et al. first proposed to use the Margules equation for ternary component mixtures in binary gas mixture adsorption, attempting to account for the adsorbate-adsorbent interactions by assuming the adsorbent as the third component. However, it was ambiguous in determining the fraction of the adsorbent and thus it was treated as an adjustable parameter. While the RASTs mentioned above need experimental data to determine parameters in the activity coefficient models, a predictive RAST (PRAST) was proposed by Sakuth et al.,<sup>15</sup> where they let the adsorption Henry's constant of a component in a binary mixture be the same as in single component adsorption. PRAST then predicted adsorbed phase activity coefficients by UNIQUAC at different fractions. Myers, from the energetic heterogeneity point of view, proposed a nonideal

adsorbed solution theory (NIAST), where attempts were made to redefine IAST.<sup>16</sup> The normalization of spreading pressure by adsorption capacity was studied in comparison with the variation of adsorption energy distribution function, and then an approach was derived from the results of molecular simulation to predict adsorbed phase activity coefficients based on a modified two-parameter Margules model. Although the original work of NIAST involved a complex study of adsorption energy distribution function, its application only requires explicit calculation which was summarized by Ushiki et al.<sup>47</sup> The NIAST has provided good predictions compared with IAST and Langmuir equation.

Although it has been extensively discussed about the deviation of IAST from experimental adsorption equilibrium and the strong spreading pressure dependency of activity coefficients,<sup>48</sup> it is not clear whether we can directly apply the same assumptions of gas mixture adsorption to aqueous phase adsorption. Erto et al. modified the original PRAST by using the Henry's constant calculated from IAST rather than from single solute adsorption to calculate infinite dilution activity coefficients, but their proposed model showed a limited success in predicting the competitive adsorption of trichloroethylene (TCE) and tetrachloroethylene (PCE).<sup>22</sup> Erto et al.<sup>8</sup> and Jadhav et al.<sup>21</sup> applied an extended Wilson equation in RAST which has an exponential function of spreading pressure as suggested by Talu and Myers<sup>48, 49</sup> for gas mixture adsorption, however, their work showed that the activity coefficients can obviously increase, decrease or only slightly change with increasing spreading pressure for TCE, PCE, and benzene derivatives on activated carbon. Thus, it is not clear how to express the variation of activity coefficient with spreading pressure.

### 2.1.2 AST Basic Thermodynamic Theory

The key assumptions in IAST for aqueous phase adsorption are: (1) all the adsorption sites are homogeneous and accessible to all solutes; (2) when there are multiple solutes with moderate adsorption capacity, all the components in the mixture behave as ideal adsorbed solutes; (3) the molar area of mixing is identical in the mixture vs. single-solute adsorption; and (4) all solutes are ideal dilute solutes and obey Henry's law. Based on these assumptions, there are five essential equations:<sup>24</sup>

$$C_i = z_i C_i^0 \quad (1)$$

$$z_i = \frac{q_i}{q^T} \quad (2)$$

$$q^T = \sum_{i=1}^n q_i \quad (3)$$

$$\frac{1}{q^T} = \sum_{i=1}^n \frac{z_i}{q_i^0} \quad (4)$$

$$\frac{\pi A}{RT} = \Psi = \int_0^{C_i^0} q_i^0 d \ln C_i^0 = \int_0^{C_i^0} \frac{q_i^0}{C_i^0} d C_i^0 = \int_0^{q_i^0} \frac{d \ln C_i^0}{d \ln q_i^0} d q_i^0 \quad (5)$$

where  $C_i$  is the equilibrium concentration of solute  $i$  in liquid phase,  $C_i^0$  is the single-solute liquid phase concentration in equilibrium with the adsorbed phase concentration  $q_i^0$  at the same temperature and spreading pressure as these of the multi-solute adsorption,  $z_i$  is the adsorbed phase fraction of solute  $i$ ,  $q^T$  is the total adsorbed phase concentration, and  $\pi$  is the spreading pressure (surface tension, surface potential, or grand potential in other literatures). The superscript <sup>0</sup> in Eqs. 1, 4, 5, and equations to follow refers to the single solute adsorption standard state. Since the total adsorption area  $A$  in

eq. (5) is not available, the reduced spreading pressure  $\Psi$  is used in the calculation, which has the same unit as adsorption capacity.<sup>49</sup>

In RAST, eqs 2-3 and 5 remain the same but eqs. 1 and 4 have been modified to:

$$C_i = z_i \gamma_i C_i^0 \quad (6)$$

$$\frac{1}{q^T} = \sum_{i=1}^n \frac{z_i}{q_i^0} + \sum_{i=1}^n \left( z_i \cdot \left[ \frac{\partial \ln \gamma_i}{\partial \Psi} \right]_{T, z_i} \right) \quad (7)$$

Adsorbed phase activity coefficients ( $\gamma_i$ ) are incorporated when the adsorbed mixtures are not ideal which violates eq. 1 (analogous to Raoult's Law).  $\gamma_i$  of less than 1 means that the experimental adsorbed concentrations are greater than the corresponding values predicted by IAST and vice versa. The partial derivatives in eq. 7 illustrate that adsorbed phase activity coefficients are functions of spreading pressure. This dependency can be neglected if the ideal solution assumptions are fulfilled, or if the molar area of mixing,  $a^m$ , is zero, which could be calculated as follows:<sup>14</sup>

$$a^m = \frac{1}{q^T} - \sum_{i=1}^n \frac{z_i}{q_i^0} = \sum_{i=1}^n \left( z_i \cdot \left[ \frac{\partial \ln \gamma_i}{\partial \Psi} \right]_{T, z_i} \right) \quad (8)$$

It was suggested that up to 30% errors could arise in determination of adsorbed amounts if this partial derivative term is wrongly neglected.<sup>14</sup>

### 2.1.3 Effects of Single Solute Adsorption Isotherm Models

Application of ASTs is not limited to any specific single-component isotherm model. Table 1 shows the most frequently used isotherm equations in IAST to simplify the model calculation: Langmuir,<sup>22, 35</sup> Freundlich,<sup>21, 35</sup> Toth,<sup>44</sup> and Dubinin-Astakhov (D-A) model.<sup>50</sup> Selection of a proper single-solute isotherm model is important because

the best IAST model prediction of adsorption of binary mixtures can only be achieved when the “best-fit” single-isotherms are applied.<sup>30, 35</sup> If the equation selected for the single-component isotherms does not precisely fit the adsorption data, IAST cannot precisely describe the adsorbed mixture.<sup>29, 47</sup> It was pointed out previously that isotherm equations in logarithm, such as Freundlich equation, D-A model, and quadratic Freundlich equation developed in this present work, are not applicable to calculating adsorbed phase Henry’s constants and reduced spreading pressure at low adsorption loading.<sup>43, 48</sup>

**Table 1.** Equations of the common single-solute isotherm models.

Name	Fitting Parameters	Equation
Langmuir	$Q^s, a_L$	$q_i = \frac{Q^s \cdot C_i}{1 + a_L \cdot C_i}$
Freundlich	$n, K$	$q_i = K \cdot C_i^{1/n}$
Toth	$Q_m, \alpha, t$	$q_i = \frac{Q_m \cdot K \cdot C_i}{[1 + (K \cdot C_i)^t]^{1/t}}$
Dubinin-Astakhov (D-A)	$Q^0, \beta, E_0$	$\text{Log } q_i = \log Q^0 - \left( \frac{-RT \ln \frac{C_i}{C_i^{sat}}}{E_0} \right)^b$
Quadratic Freundlich	$m, n, K$	$\ln q_i = m \cdot (\ln c_i)^2 + n \cdot \ln c_i + \ln K$
Dual-site Langmuir (DSL)	$Q_A^s, Q_B^s, b_A, b_B$	$q_i = \left( \frac{Q_A^s c_i}{1 + b_A c_i} \right)_{site A} + \left( \frac{Q_B^s c_i}{1 + b_B c_i} \right)_{site B}$

Note: For all models,  $C_i$  is the equilibrium solution concentration,  $q_i$  is the equilibrium adsorbed concentration, and  $C_i^{sat}$  is the solute aqueous solubility

### 2.1.4 Activity Coefficients of Adsorbates in Adsorbed Mixtures

The widely accepted fundamental thermodynamic restrictions of adsorbed phase activity coefficients  $\gamma_i(\Psi, z_i)$  are as follows<sup>15</sup>

1.  $\gamma_i(\Psi, z_i)$  of component i approaches unity when  $z_i$  approaches unity.

$$\lim_{z_i \rightarrow 1.0} \gamma_i(\Psi) = 1.0 \quad (9)$$

2. As the spreading pressure, e.g. the total adsorption loading, approaches zero,  $\gamma_i(\Psi, z_i)$  approaches unity for all components.

$$\lim_{\Psi \rightarrow 0} \gamma_i = 1.0 \quad (10)$$

3. When a non-logarithmic isotherm equation is used,  $\gamma_i(\Psi, z_i)$  approaches the infinite dilution value  $\gamma_i^\infty$ .

$$\lim_{z_i \rightarrow 0} \gamma_i(\Psi) = \gamma_i^\infty(\Psi) \quad (11)$$

Two key problems of  $\gamma_i(\Psi, z_i)$  are the spreading pressure dependency and infinite dilution values. One of the most prevailing factor of spreading pressure dependency for  $\ln \gamma_i$  is  $(1 - e^{-c \cdot \Psi})$  where c is an adjustable parameter.<sup>49</sup>

## 2.2 Segregated Adsorption Models

In dealing with nonideality of adsorbed phase mixtures, another approach is to assume heterogeneous adsorption sites, or energetic heterogeneity.<sup>17, 32</sup> The dual-site Langmuir model (DSL) was first derived to study activity coefficients of adsorbates by assuming segregated adsorption sites.<sup>20</sup> It assumes that adsorbates form ideal adsorbed

solution on two independent sites. When all solutes have the same adsorption capacity at saturation on each site, the DSL model is identical to applying IAST at each site. Later, this segregated idea was further developed as heterogeneous IAST (HIAST) by assuming that each component has a distribution of adsorption sites.<sup>17, 32</sup> However, a proper adsorption energy distribution function must be assumed in advance and be further parameterized. Attempts have been made by Myers in developing NIAST to correlate the heterogeneity back to activity coefficients.<sup>16</sup> Since NIAST was derived based on molecular simulation involving only the difference in size of the adsorbate molecules, it only shows a limited success in predicting the adsorption of volatile organic molecules on activated carbon.<sup>47</sup> More recently, the dual-site Langmuir model was brought back to the stage for multicomponent adsorption.<sup>18, 19</sup> For instance, Ritter et al. attempted to account for nonideality by using a multi-component dual-site Langmuir (MSDSL) model, where binary/ternary components were allowed to have different maximum adsorption capacities on each site. Thus, MSDSL is not thermodynamically consistent and is not identical to IAST anymore.<sup>20</sup> Swisher et al. attempted to keep thermodynamic consistency by using the original IAST on both sites while still allowing differences in adsorption saturation, which is termed segregated IAST (SIASST).<sup>18</sup> To our best knowledge, none of these models, HIAST, MSDSL, and SIASST, have been used for multi-solute adsorption in the aqueous phase. In the present work, MSDSL and SIASST were applied to make comparison with IAST.

### 2.3 Multi-solute Adsorption

Although intensive research has been conducted on the single-solute adsorption of benzene derivatives such as nitrobenzene, anilines, phenols, and polycyclic aromatics, there is only limited effort examining competitive adsorption in multi-solute systems. Zhang W.M. et al. and Valderrama et al. studied the binary adsorption of phenol/aniline onto MN200 and GAC using the extended Langmuir and Freundlich equations.<sup>51,52</sup> In another work of Zhang W.M. et al., it was shown that Lewis acid-base interactions should be considered to account for the adsorption enhancement of aniline and phenol.<sup>27</sup> Yang et al. proposed a surface-dominated sorption mechanism in the study of competitive adsorption of pyrene, phenanthrene, and naphthalene,<sup>26,28</sup> but IAST was proved to be insufficient in predicting the adsorption equilibrium of the primary solute.<sup>26</sup> We note that the concentrations of the competitors were too close to their water solubility in the above work so that it is expected that IAST gave poor prediction in such systems.

Sander et al. studied adsorbate-adsorbent interactions in competitive adsorption by normalization of hydrophobic effects and concluded that  $\pi$ - $\pi$  electron donor-acceptor (EDA) interactions with multi-walled carbon nanotubes provided extra forces for the adsorption of nitrobenzene compared to that of toluene and benzene.<sup>53</sup> Jadhav et al. combined RAST with the modified Wilson equation in modeling binary adsorption of nitrobenzene, aniline, and phenol.<sup>21</sup> Linear relationships were reported in their work between the activity coefficients of the two solutes with a constant concentration ratio. However, the linear relationships were obtained based on regression analysis for each test at each constant ratio, and thus, they are not ready to be applied to other solute

concentration ratios that have not been tested. Abburi<sup>54</sup> has conducted both batch and column adsorption experiments to remove phenol and p-chlorophenol by Amberlite XAD-16 using the IAST method proposed by Crittenden et al<sup>24</sup>. A pH of 6 was found to be feasible for the bisolute adsorption and the resin was found to be able to remove phenols in repeated column test. Sulaymon et al. studied the equilibrium and dynamic column adsorption of furfural and phenolic compounds on activated carbon using a general multicomponent rate model which considers axial dispersion, external mass transfer, and intraparticle diffusion resistance.<sup>55</sup> The simple multicomponent Langmuir model was used to determine the competitive adsorption equilibrium with close agreements between the simulated breakthrough curves and the experimental results for bi- and tri-solute adsorption of furfural, phenol, and p-chlorophenol. Valderrama et al. showed faster regeneration and a high percentage of recovery of MN200 in the removal of aniline and phenol while their prediction of breakthrough curves also agreed with experimental results.<sup>56</sup> Valderrama et al. also showed that IAST performs better than multicomponent Langmuir model in determining the adsorption equilibrium which was then applied in fixed-bed adsorption models to predicting adsorption breakthrough curves for aniline and phenol.<sup>9</sup> However, in all three studies just mentioned, the concentration ratios of solutes were close to 1:1, which is not very common in real water treatment systems. Since the accurate data of multicomponent adsorption equilibrium is necessary for fixed-bed column adsorption, an accurate model is desirable for solute mixtures with variable concentration ratios.

## 2.4 Polymeric Resin Adsorbent

Polymeric resins typically have high surface area, small pore size, and adjustable selectivity for OCs.<sup>57</sup> A number of studies have shown that resins are effective in removing a variety of OCs such as phenols, anilines, organic acids, aromatic hydrocarbons, alkanes and selected pesticides from aqueous solution.<sup>57-66</sup> Resins also have facile regeneration under mild conditions (e.g., hot water, weak acid/base, and organic solvents) and stable performance over a long period; these features have enabled their full-scale application to various industrial wastewater treatment.<sup>57, 62, 66</sup> In addition, resins can maintain their structural integrity and adsorption performance after more than 2,000 regeneration cycles, as opposed to AC that typically needs to be replaced after 15 to 20 cycles.<sup>66</sup> There are two major types of resins used in industrial wastewater treatment: polystyrenes and polyacrylic esters.<sup>67</sup> Comparably, polystyrene resins are more selective toward aromatic OCs while polyacrylic resins are more hydrophilic and attract more polar OCs.<sup>57</sup> Based on adsorbate-adsorbent interaction forces ranging from induced dipole related interactions to  $\pi$ - $\pi$  interactions to H-bonding, the recent work of our group has successfully developed predictive models that can estimate adsorption isotherms of various single aromatic contaminants by three widely used neutral resins: MN200 (microporous polystyrene), XAD4 (porous polystyrene) and XAD7 (porous polyacrylic).<sup>68-70</sup>

## CHAPTER 3

### EXPERIMENTAL AND MODELING APPROACH

#### 3.1 Adsorption isotherms

##### 3.1.1 Solutes and Adsorbent

Macronet MN200, a hyper-crosslinked nonionic polymeric resin was obtained from Purolite® (U.S.). Before batch adsorption experiments, the resin was subjected to NaOH/DI-water/HCl wash, followed by extraction with methanol in a Soxhlet apparatus to remove residual impurities. All selected solutes including nitrobenzene (99+%), aniline (99+%), 4-nitroaniline (99+%), 4-chloroaniline (99+%), phenol (99+%), 4-chlorophenol (99+%), 4-methylphenol (99+%), and 4-nitrophenol (99+%) were purchased from Fisher Scientific and prepared in DI water without further purification. Physical-chemical properties of selected aromatic compounds are shown in **Table 2**.

**Table 2.** Physical-chemical properties of selected aromatic compounds

Compounds	Abbr.	C <sup>sat</sup> (mM)	log K <sub>HW</sub>	log K <sub>gw</sub>	pK <sub>a</sub>	Melting point (°C)
Nitrobenzene	NB	16.982	1.54	-3.12	/	5.7
Aniline	/	386.556	-0.04	-4.03	4.63	-6.0
4-Nitroaniline	4-NA	5.792	-1.2	-7.18	1.0	146
4-Chloroaniline	4-CA	21.596	0.56	-4.35	4.15	72.5
Phenol	/	852.088	-1.08	-4.59	9.89	40.9
4-Chlorophenol	4-CP	204.574	-0.75	-5.05	9.18	42.7
4-Methylphenol	4-MP	175.714	-0.19	-4.15	10.17	35.5
4-Nitrophenol	4-NP	115.025	-1.93	-7.66	7.15	113

Note: C<sup>sat</sup> is the aqueous solubility from ref <sup>68</sup>, K<sub>HW</sub> is the n-hexadecane-water partitioning coefficient from ref <sup>68</sup>, K<sub>GW</sub> is the Henry's constant for gas-water equilibrium

from ref <sup>68</sup>,  $pK_a$  is the negative of the logarithm of dissociation constants of phenols and ammonium ions of corresponding anilines from refs <sup>71,72</sup> and M.P. stands for melting point from ref <sup>73</sup>.

These 8 aromatic compounds were chosen to represent diverse intermolecular interactions as reflected by their different aqueous solubility,  $K_{HW}$  and  $pK_a$ . Because steric effects were not the focus of this work, many of these compounds were chosen to contain para positioned substituents. Based on  $\pi$ -electron withdrawing and donating effects, these compounds can be divided into three groups: (1) phenol, aniline, and 4-MP are  $\pi$ -electron sufficient; (2) 4-CP and 4-CA are treated as weakly  $\pi$ -electron sufficient; and (3) NB, 4-NP, and 4-NA are  $\pi$ -electron deficient.

### **3.1.2 Batch Adsorption Experiments**

The adsorption experiments were performed in amber glass bottles equipped with Teflon-lined screw caps at  $23 \pm 0.5^\circ\text{C}$ . The pH values were about neutral for 4-MP, aniline, phenol, 4-CP, 4-CA, NB and 4-NA, and  $4.0 \pm 0.5$  for 4-NP. The bottles with different solute-sorbent combinations were then transferred to a shaker equipped with a thermostat under 175 rpm for 48 hrs. Initial and equilibrium concentrations were determined by HPLC with methanol and distilled water (methanol and pH=3.0 phosphoric acid) as mobile phase. For binary-solute adsorption, at least 90 seconds of difference in the retention times of each pair of solutes were obtained by changing the ratio of methanol and distilled water (or pH=3.0 phosphoric acid).

### 3.1.3 Error Analysis

The correlation of calculated values,  $V_i^{calc}$ , by fitting equations of adsorption isotherms or activity coefficients with experimental values,  $V_i^{exp}$ , was evaluated using statistic equations such as relative error (RE, eq. 12), root mean square error (RMSE, eq. 13), and mean weighted square error (MWSE, eq. 14). All adjustable parameters in fitting equations for adsorption isotherms and activity coefficients were determined by the least-square error method (LSE, eq. 15).

$$RE = \left| \frac{V_i^{exp} - V_i^{calc}}{V_i^{calc}} \right| \times 100\% \quad (12)$$

$$RMSE = \sqrt{\frac{1}{n} \sum_n \left( \left| \frac{V_i^{exp} - V_i^{calc}}{V_i^{calc}} \right|^2 \right)} \times 100\% \quad (13)$$

$$MWSE = \frac{1}{n-3} \sum_n \left( \left| \frac{V_i^{exp} - V_i^{calc}}{V_i^{calc}} \right|^2 \right) \times 100\% \quad (14)$$

$$LSE = \frac{1}{n} \sum_n \left( \left| \frac{V_i^{exp} - V_i^{calc}}{V_i^{calc}} \right|^2 \right) \times 100\% \quad (15)$$

### 3.1.4 Selection of Single Solute Models

Single solute adsorption data from previous work in our research group is plotted in Figure 1.<sup>69</sup> Our preliminary work showed that for the single-solute adsorption isotherms of aniline, phenol, and their substitutes by MN200, an empirical equation developed by ourselves (i.e. the quadratic Freundlich in Table 1) and Toth equation gave much smaller MWSEs than D-A model (Table 2).<sup>69</sup> In this study, the quadratic Freundlich equation was chosen to implement algorithm of ASTs rather than Toth

equation since Toth equation has to be numerically integrated.<sup>74</sup> Dual-site Langmuir equation was applied in Segregated IAST (SIAST) and multi solute dual-site Langmuir (MSDSL) models.<sup>18, 19</sup>

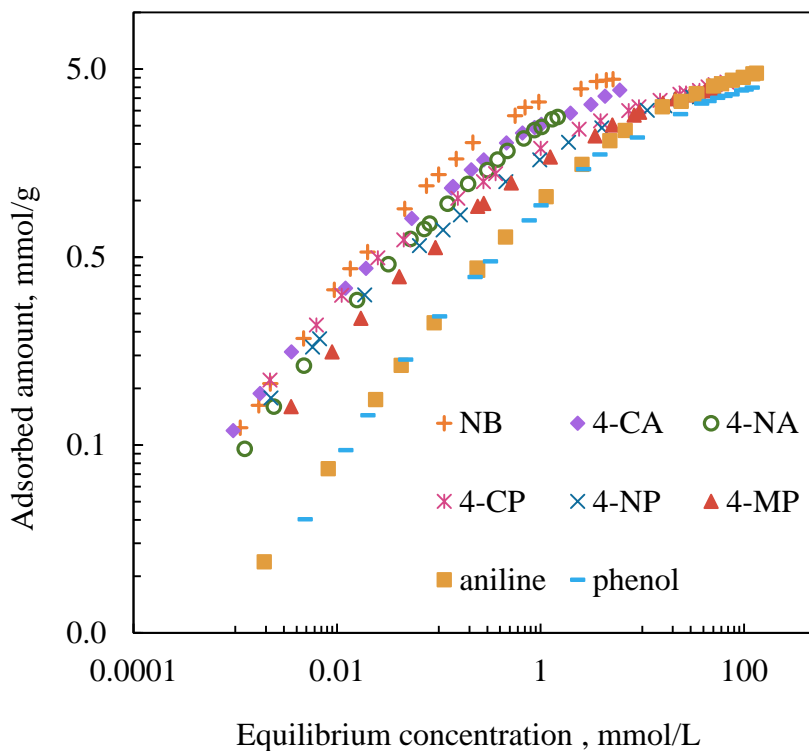


**Figure 1.** Experimental data of single solute adsorption of 8 aromatic compounds onto MN200. Adapted from ref<sup>69</sup>

**Table 3.** Fitting results of single-solute isotherm models

Compound (abbr.)	Quadratic Freundlich				Toth				D-A				Dual-site Langmuir				
	m	n	K	MWSE	$Q_m$	$\alpha$	t	MWSE	$Q_0$	$E_0$	$\beta$	MWSE	$Q_A^S$	$b_A$	$Q_B^S$	$b_B$	MWSE
NB	-0.0485	0.267	1.193	1E-03	6.49	10.91	0.438	1E-03	4.645	17.2	2.17	1E-02	4.04	2.36	0.67	62.37	2E-03
Phenol	-0.0404	0.498	-0.090	6E-04	6.23	1.02	0.361	8E-04	4.456	20.05	2.08	2E-03	3.51	0.17	0.38	9.23	3E-03
4-MP	-0.0306	0.348	0.455	5E-04	7.04	11.71	0.274	4E-04	4.197	20.39	1.8	4E-03	3.26	0.21	0.84	21.31	8E-03
4-CP	-0.0266	0.292	0.652	1E-03	6.72	40.73	0.258	4E-04	4.426	22.98	1.75	1E-02	3.06	0.28	1.06	36.05	4E-04
4-NP	-0.0263	0.313	0.495	4E-04	7.66	33.96	0.234	7E-04	3.806	20.57	1.81	1E-03	3.03	0.54	0.60	61.08	5E-03
Aniline	-0.0347	0.502	-0.038	2E-03	9.25	0.93	0.314	1E-03	5.023	17.82	1.88	2E-03	4.19	0.12	0.51	7.25	1E-02
4-CA	-0.0349	0.297	0.918	6E-04	8.05	18.58	0.298	6E-04	4.205	17.77	1.77	2E-03	3.38	1.50	0.65	84.64	5E-03
4-NA	-0.0305	0.383	0.895	3E-04	15.92	6.68	0.256	3E-04	3.763	13.59	1.48	1E-03	3.40	1.48	0.44	75.10	1E-03

### 3.1.5 Solution of IAST

In binary systems, there is a set of four equations based on eqs 1-5 for IAST<sup>12, 24</sup>

$$C_1 - \frac{q_1}{q_1+q_2} C_1^0 = 0 \quad (16)$$

$$C_2 - \frac{q_2}{q_1+q_2} C_2^0 = 0 \quad (17)$$

$$\frac{q_1}{q_1^0} + \frac{q_2}{q_2^0} - 1 = 0 \quad (18)$$

$$\Psi_1(C_1^0) - \Psi_2(C_2^0) = 0 \quad (19)$$

For different single solute isotherms,  $\Psi_i$  ( $i = 1, 2$ ) can be explicit functions of either  $C_i^0$  or  $q_i^0$  (refer to eq. 5). By substituting the quadratic Freundlich equation

$$q_i^0 = \exp(m_i \cdot (\ln C_i^0)^2 + n_i \cdot \ln C_i^0 + \ln K_i) \quad (20)$$

into eq. 5 we obtain:

$$\Psi_i(C_i^0) = \frac{0.5\sqrt{P_i} \cdot e^{\frac{4m_i \ln K_i - n_i^2}{4m_i}} \cdot (1 - \operatorname{erf}(\frac{2m_i \ln C_i^0 + n_i}{2\sqrt{-m_i}}))}{\sqrt{-m_i}}, \quad P_i = 3.14159 \quad (21)$$

Then, by substitute eq. 20 into Eq. 18 and eq. 21 into eq. 19, we constitute the 4 nonlinear simultaneous equations with two unknown  $C_i^0$  values and two unknown  $q_i$  values.

$$F_1 = C_1 - \frac{q_1}{q_1+q_2} C_1^0 = 0 \quad (22)$$

$$F_2 = C_2 - \frac{q_2}{q_1+q_2} C_2^0 = 0 \quad (23)$$

$$F_3 = \frac{q_1}{e^{m_1(\ln C_1^0)^2 + n_1 \ln C_1^0 + \ln K_1}} + \frac{q_2}{e^{m_2(\ln C_2^0)^2 + n_2 \ln C_2^0 + \ln K_2}} - 1 = 0 \quad (24)$$

$$F_4 = \frac{0.5\sqrt{P_i} \cdot e^{\frac{4m_1 \ln K_1 - n_1^2}{4m_1}} \cdot (1 - \operatorname{erf}\left(\frac{2m_1 \ln C_1^0 + n_1}{2\sqrt{-m_1}}\right))}{\sqrt{-m_1}} - \frac{0.5\sqrt{P_i} \cdot e^{\frac{4m_2 \ln K_2 - n_2^2}{4m_2}} \cdot (1 - \operatorname{erf}\left(\frac{2m_2 \ln C_2^0 + n_2}{2\sqrt{-m_2}}\right))}{\sqrt{-m_2}} = 0 \quad (25)$$

The unknowns for eqs. 22-25 are  $C_i^0$  and  $q_i$ . If we let the solution be  $X = (q_1, q_2, C_1^0, C_2^0)'$  (the prime is known as transpose), the 4 nonlinear simultaneous equations can be solved numerically by Newton-Raphson iteration, which is formulated as follows

$$\vec{X}_{new} = \vec{X}_{ini} - J_{ini}^{-1} \vec{F}_{ini} \quad (26)$$

where  $\vec{X}_{initial}$  is the initial guess of the solution and  $\vec{X}_{new}$  is the new solution.  $J_{ini}^{-1}$  is the inverse matrix of Jacobian matrix, J, as shown in eq. 27.

$$J = \begin{pmatrix} \frac{\partial F_1}{\partial q_1} & \frac{\partial F_1}{\partial q_2} & \frac{\partial F_1}{\partial C_1^0} & \frac{\partial F_1}{\partial C_2^0} \\ \frac{\partial F_2}{\partial q_1} & \frac{\partial F_2}{\partial q_2} & \frac{\partial F_2}{\partial C_1^0} & \frac{\partial F_2}{\partial C_2^0} \\ \frac{\partial F_3}{\partial q_1} & \frac{\partial F_3}{\partial q_2} & \frac{\partial F_3}{\partial C_1^0} & \frac{\partial F_3}{\partial C_2^0} \\ \frac{\partial F_4}{\partial q_1} & \frac{\partial F_4}{\partial q_2} & \frac{\partial F_4}{\partial C_1^0} & \frac{\partial F_4}{\partial C_2^0} \end{pmatrix} \quad (27)$$

where

$$\frac{\partial F_i}{\partial q_i} = -\frac{C_i^0}{q_i + q_j} + \frac{q_i C_i^0}{(q_i + q_j)^2} \quad (28)$$

$$\frac{\partial F_i}{\partial q_j} = \frac{q_i C_i^0}{(q_i + q_j)^2} \quad (29)$$

$$\frac{\partial F_i}{\partial C_i^0} = -\frac{1}{q_i + q_j} \quad (30)$$

$$\frac{\partial F_i}{\partial C_j^0} = 0 \quad (31)$$

$$\frac{\partial F_3}{\partial q_i} = \frac{1}{e^{m_i(\ln C_i^0)^2 + n_i \ln C_i^0 + \ln K_i}} \quad (32)$$

$$\frac{\partial F_3}{\partial C_i^0} = (-1)^{i-1} \frac{q_i \left( \frac{2m_i \ln C_i^0}{C_i^0} + \frac{n_i}{C_i^0} \right)}{e^{m_i(\ln C_i^0)^2 + n_i \ln C_i^0 + \ln K_i}} \quad (33)$$

$$\frac{\partial F_4}{\partial q_i} = 0 \quad (34)$$

$$\frac{\partial F_4}{\partial C_i^0} = (-1)^{i-1} \frac{e^{m_i(\ln C_i^0)^2 + n_i \ln C_i^0 + \ln K_i}}{C_i^0} \quad (35)$$

$i = 1$  or  $2, j = 1$  or  $2$  and  $i \neq j$  for eqs 28-35.

From each initial guess of  $\vec{X}_{ini}, \vec{F}_{ini} = (F_1, F_2, F_3, F_4)'$  could be calculated, so as  $J_{ini}^{-1}$ . Then  $\vec{X}_{new}$  was calculated by eq. 26 and set as  $\vec{X}_{ini}$  for the next iteration. The same iteration process was repeated until eqs. 22 to 25 were satisfied. Once all unknowns were calculated, the reduced spreading pressure was determined by eq. 21.

In the present work, the initial guesses of the unknowns,  $q_1^{ini}, q_2^{ini}, C_1^{0,ini}$ , and  $C_2^{0,ini}$ , were obtained by the following empirical method we developed. By using this method, the iteration of Newton-Raphson algorithm always converged with few failures under varying conditions such as initial concentration ratios of up to 1:100.

First, the concentration of component i,  $C_i$ , was converted to an equivalent concentration of component j,  $C_{i,j}$ , by assuming that they are equally competitive if their equilibrium adsorbed amounts are the same in single solute adsorption equilibrium (eqs. 36 and 37). eq. 37 is simply the inverse function of the quadratic Freundlich equation.

$$q_i' = e^{(m_i \cdot (\ln C_i)^2 + n_i \cdot \ln C_i + \ln K_i)} \quad (36)$$

$$C_{i,j} = e^{\frac{-n_j + (n_j^2 - 4m_j(\ln K_i - \ln q_i'))^{0.5}}{2m_j}} \quad (37)$$

Then, the binary solute mixture becomes a mixture of the real solute j with concentration  $C_j$  and the hypothetical solute j with concentration  $C_{i,j}$  converted from solute i. The initial guesses of  $q_j^{ini}$  were then determined from eqs. 38-40

$$C_j^T = C_j + C_{i,j} \quad (38)$$

$$q_j^T = e^{(m_j \cdot (\ln C_j^T)^2 + n_j \cdot \ln C_j^T + \ln K_j)} \quad (39)$$

$$q_j^{ini} = \frac{C_j q_j^T}{C_j^T} \quad (40)$$

eq. 40 was derived by assuming identical fractions of solute j in the adsorbed phase and the aqueous phase. For each component, we had to repeat the conversion (eq. 36 and eq. 37) first and then calculate  $C_j^T$ ,  $q_j^T$  and  $q_j^{ini}$ . Once we had all  $q_j^{ini}$  values,  $C_j^{0,ini}$  values were determined by eq. 41 which was derived from eq. 1

$$C_j^{0,ini} = \frac{C_j \sum q_j^{ini}}{q_j^{ini}} \quad (41)$$

### 3.1.6 Multi Solute Dual-Site Langmuir (MSDSL)

For the assumed two-site heterogeneous surface consisting of site A and site B, the single solute adsorption isotherm is

$$q_i = \left( \frac{Q_{A,i}^s c_i}{1+b_{A,i} c_i} \right)_{site A} + \left( \frac{Q_{B,i}^s c_i}{1+b_{B,i} c_i} \right)_{site B} \quad (42)$$

The site that component i has a higher adsorption energy is always denoted as site A.

We used the same site-matching approach of Ritter et al. and assumed that in all binary adsorption, primary component A and competitor B follow a perfect positive correlation, that is, both solutes have higher adsorption energy on site A.<sup>19</sup> Thus, the binary solute dual-site Langmuir model is given as

$$q_1 = \left( \frac{Q_{A,1}^s c_1}{1+b_{A,1} c_1+b_{A,2} c_2} \right)_{site A} + \left( \frac{Q_{B,1}^s c_1}{1+b_{B,1} c_1+b_{B,2} c_2} \right)_{site B} \quad (43)$$

$$q_2 = \left( \frac{Q_{A,2}^s c_2}{1+b_{A,2} c_2+b_{A,1} c_1} \right)_{site A} + \left( \frac{Q_{B,2}^s c_2}{1+b_{B,2} c_2+b_{B,1} c_1} \right)_{site B} \quad (44)$$

Components A and B could have different saturation capacity on the same site from the fitting point of view. However, only when  $Q_{A,1}^s$  is identical to  $Q_{A,2}^s$ , and  $Q_{B,1}^s$  to  $Q_{B,2}^s$ , then eqs 43 and 44 are thermodynamically consistent.<sup>20</sup>

### 3.1.7 Segregated Ideal Adsorbed Solution Theory (SIASST)

Single solute adsorption isotherms were fitted into eq. 42. The same fitting parameters and site-matching approach as in MSDSL are accepted in SIASST. While in MSDSL the adsorbed amounts were predicted by eq. 43 and eq. 44, IAST was implemented separately at the two segregated adsorption sites in SIASST to predict the competitive adsorption at each site.

Eq. 45 relates the reduced spreading pressure for single solute adsorption of component  $i$  ( $i=1$  or  $2$ ) at site  $k$  ( $k=A$  or  $B$ ) to the Langmuir adsorption isotherm based on eq. 5.

$$\Psi_{k,i} = \int_0^{C_{k,i}^0} q_{k,i}^0 d \ln C_{k,i}^0 = Q_{k,i}^s \ln(1 + b_{k,i} C_{k,i}^0) \quad (45)$$

where  $q_{k,i}^0$  is the single-solute adsorbed phase concentration of component  $i$  at site  $k$  with the same spreading pressure as the mixture.

$$q_{k,i}^0 = \frac{Q_{k,i}^s C_{k,i}^0}{1 + b_{k,i} C_{k,i}^0} \quad (46)$$

Then the 4 nonlinear simultaneous equations were constituted separately for site  $k$  by substituting eq. 40 into eq. 14 and eq. 41 in eq. 13 as follows

$$F_{k,1} = C_1 - \frac{q_{k,1}}{q_{k,1} + q_{k,2}} C_{j,1}^0 = 0 \quad (47)$$

$$F_{k,2} = C_2 - \frac{q_{k,2}}{q_{k,1} + q_{k,2}} C_{j,2}^0 = 0 \quad (48)$$

$$F_{k,3} = \frac{q_{k,1}(1 + b_{k,1} C_1)}{Q_{k,1}^s C_1} + \frac{q_{k,2}(1 + b_{k,2} C_2)}{Q_{k,2}^s C_2} - 1 = 0 \quad (49)$$

$$F_{k,4} = Q_{k,1}^s \ln(1 + b_{k,1} C_{k,1}^0) - Q_{k,2}^s \ln(1 + b_{k,2} C_{k,2}^0) = 0 \quad (50)$$

where  $q_{k,i}$  is the unknown adsorbed amount of component  $i$  at site  $k$ .  $q_{A,i}$  and  $q_{B,i}$  were separately calculated from two sets of equations for site A and site B. We can then express the total adsorbed amount of component  $i$  as

$$q_i = q_{A,i} + q_{B,i} \quad (51)$$

The initial guesses of  $q_{k,i}$  for site k were obtained based on the results of MSPDL for site k (eq. 52).

$$q_{k,i} = \left( \frac{Q_{k,i}^s C_i}{1 + b_{k,i} C_i + b_{k,j} C_j} \right) \quad (52)$$

Initial values of  $C_{j,i}^0$  were calculated based on eqs. 1-3.

### 3.1.8 Design of Binary Adsorption Experiments

All sets of binary solute adsorption data were collected from batch adsorption experiments. Initial concentrations of both components, solution volume, and dosage of MN200 resin were designed to fulfill the following rules:

1. Expected equilibrium concentrations of component A, denoted as the primary solute, changed approximately from 0.005mM to 40mM or about 40% of the saturation concentration.
2. Expected equilibrium concentrations of component B, denoted as the competitor, were set at a constant value.
3. The adsorbed amounts of the primary solute and the competitor were predicted by IAST using the expected equilibrium concentrations of components A and B. By changing the expected equilibrium concentration, we were able to change the expected adsorbed amounts and thus, let the adsorbed phase mole fractions change from 0.1 to 0.9.
4. Either 20mL or 50mL of total volume was chosen in batch experiments based on the concentration of the primary solute.

5. Initial concentrations of the primary solute and the competitor were calculated from batch adsorption mass balance (eq. 53) while the dosage of the adsorbent was adjusted to obtain a constant initial concentration of the competitor.

$$C_{ini,i} - C_i = \frac{Mq_i}{V} \quad (53)$$

At adsorption equilibrium, the concentration of the competitor was not exactly a constant due to the deviation of IAST from experimental equilibrium, but decreased by 1% to 10% as the concentration of the primary solute increased.

### 3.2 Real adsorbed Solution Theory (RAST) and $\gamma_i$ Modeling

#### 3.2.1 Calculation of $\gamma_i$ Based on Experimental Data

To evaluate reduced spreading pressure in binary solute adsorption equilibrium, the Gibbs adsorption equation

$$d\Psi = d\left(\frac{\pi A}{RT}\right) = \sum_i^n q_i d\ln C_i \quad (54)$$

or

$$d\Psi = d\left(\frac{\pi A}{RT}\right) = q_T d\ln C_T + \sum_i^n C_T z_i d\ln x_i \quad (55)$$

had to be integrated from zero loading to experimental equilibrium conditions of our interests, where

$$C_T = \sum_i^n C_i \quad (56)$$

$$x_i = \frac{C_i}{C_T} \quad (57)$$

For binary adsorption equilibrium in batch reactors, as mentioned before, the initial concentration can be held as constant but accurate control on the equilibrium concentration is not always available. Thus, three methods for binary adsorption in batch reactors are expressed in this work as follows

- i. Constant ratio of the initial concentrations of the two components

As preliminary results and previous work of other researches show, if the two components have a constant ratio of the initial concentrations, then the equilibrium concentrations obey a linear logarithmic correlation which can be expressed as (**Figure 2**)

$$\ln C_1 = A \ln C_2 + B \quad (58)$$

and

$$d \ln C_1 = A d \ln C_2 \quad (59)$$

Then, eq. 48 is integrated as

$$\Psi = \int_0^{C_1} (Aq_1 + q_2) d \ln C_1 = \int_0^{C_2} (q_1 + \frac{q_2}{A}) d \ln C_2 \quad (60)$$

- ii. Constant initial concentration of the competitor

The equilibrium concentration of the competitor usually decreases by 1% to 15% from the expected equilibrium concentration as the concentration of the primary solute increases. This is due to the underestimation of the adsorbed amount of the competitor by IAST when its fraction decreases from 1.00 to 0.00. We derived the integral of eq. 54 by assuming the equilibrium concentration of the competitor is constant. This method is expressed as the following equation and also as the two-step integration path (BR1) in

Figure 2

$$\Psi = \int_0^{C_2} q_2^0(0, C_2^0) d\ln C_2^0 + \int_0^{C_1} q_1(C_1, C_2^{const}) d\ln C_1 = \Psi_I + \Psi_{II} \quad (61)$$

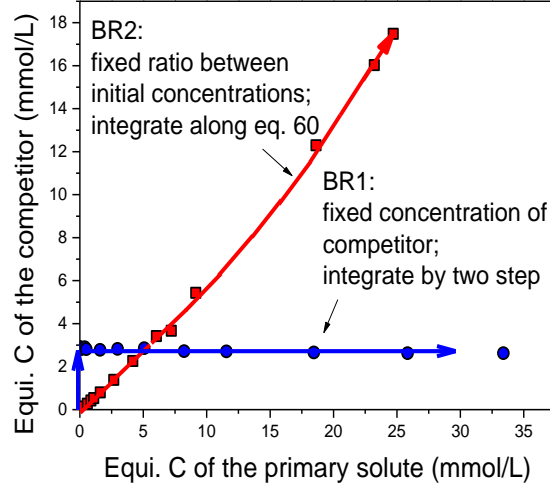


**Figure 2.** Two proposed integration paths for eq. 54

The first integral term in eq. 61 is the integration of the single component isotherm of the competitor from zero loading to its equilibrium concentration in binary adsorption,  $C_2$ . The second integral term in eq. 61 is the integration of the experimental isotherm of the primary solute in the bisolute mixture from zero to its equilibrium concentration,  $C_1$ , where  $q_1(C_1, C_2^{const})$  is the fitting on the quadratic Freundlich equation of the adsorption isotherm of the primary solute in the presence of an approximately constant concentration of the competitor,  $C_2^{const}$ . After substituting eq. 21 into eq. 61, we express the result as follows

$$\Psi_I = \int_0^{C_2} q_1(0, C_2) d\ln C_2 = \frac{0.5\sqrt{Pi} \cdot e^{\frac{4 m_2 \ln K_2 - n_2^2}{4m_2}} \cdot \left(1 - \operatorname{erf}\left(\frac{2m_2 \ln C_2^0 + n_2}{2\sqrt{-m_2}}\right)\right)}{\sqrt{-m_2}} \quad (62)$$

$$\Psi_{II} = \int_0^{C_1} q_1(C_1, C_2^{const}) d\ln C_1 = \frac{0.5\sqrt{Pi} \cdot e^{\frac{4 m_{1,exp} \ln K_{2,exp} - n_{2,exp}^2}{4m_{1,exp}}} \cdot \left(1 - \operatorname{erf}\left(\frac{2m_{1,exp} \ln C_1 + n_{2,exp}}{2\sqrt{-m_{1,exp}}}\right)\right)}{\sqrt{-m_{1,exp}}} \quad (63)$$

$$\Psi = \Psi_I + \Psi_{II} \quad (64)$$

In eq. 62, parameters  $m_2$ ,  $n_2$  and  $K_2$  are from single solute adsorption of the competitor.

In eq. 63, parameters  $m_{1,exp}$ ,  $n_{1,exp}$ , and  $K_{1,exp}$  are from the experimental data of the binary solute adsorption of the primary solute.

With the experimental  $\Psi$  values calculated by eq. 64,  $C_1^0$  and  $C_2^0$  were numerically determined from eq. 21 by letting  $\Psi_i(C_i^0)$  equal to  $\Psi$ . Then the experimental  $\gamma_i$  values,  $\gamma_i^{exp}$ , can be calculated as follows

$$\gamma_i^{exp} = \frac{C_i}{z_i C_i^0} \quad (65)$$

The four simultaneous nonlinear equations of RAST using  $\gamma_i^{exp}$  are expressed as

$$F_1 = C_1 - \frac{q_1}{q_1 + q_2} \gamma_1^{exp} C_1^0 = 0 \quad (66)$$

$$F_2 = C_2 - \frac{q_2}{q_1 + q_2} \gamma_2^{exp} C_2^0 = 0 \quad (67)$$

$$F_3 = \frac{q_1}{e^{m_1(\ln C_1^0)^2 + n_1 \ln C_1^0 + \ln K_1}} + \frac{q_2}{e^{m_2(\ln C_2^0)^2 + n_2 \ln C_2^0 + \ln K_2}} - 1 = 0 \quad (68)$$

$$F_4 = \frac{0.5\sqrt{P}i \cdot e^{\frac{4m_1 \ln K_1 - n_1^2}{4m_1}} \cdot \left(1 - \operatorname{erf}\left(\frac{2m_1 \ln C_1^0 + n_1}{2\sqrt{-m_1}}\right)\right)}{\sqrt{-m_1}} - \frac{0.5\sqrt{P}i \cdot e^{\frac{4m_2 \ln K_2 - n_2^2}{4m_2}} \cdot \left(1 - \operatorname{erf}\left(\frac{2m_2 \ln C_2^0 + n_2}{2\sqrt{-m_2}}\right)\right)}{\sqrt{-m_2}} = 0 \quad (69)$$

Since  $\gamma_i$  is assumed to be independent on spreading pressure, the partial derivative term in eq. 7 is neglected in eq. 68.

iii. Infinite dilute solution of the primary solute

When the primary solute has much lower concentrations in both the aqueous phase and the adsorbed phase than the competitor, the following approximation can be made:

$$z_1 = \lim_{\frac{q_1}{q_2} \rightarrow 0} \frac{q_1}{q_1 + q_2} = \frac{q_1}{q_2} \quad (70)$$

This infinite dilute condition for adsorbed binary mixtures resembles the infinite dilute condition of liquid mixtures by viewing the adsorbed primary solute as an infinite dilute solute and the adsorbed competitor as a bulk phase of solvent. In such a case, it is reasonable to assume that the adsorption equilibrium of the competitor is close to its single-solute adsorption system. Therefore, eq. 70 can be further approximated as:

$$z_1 = \lim_{q_1 \rightarrow 0} \frac{q_1}{q_1 + q_2} \approx \frac{q_1}{q_2^0} \quad (71)$$

By substituting eq. 71 into eq. 65, we obtain

$$\gamma_1^\infty = \frac{c_1 q_2^0}{q_1 C_1^0} \quad (72)$$

and

$$q_1 = \frac{c_1 q_2^0}{\gamma_1^\infty C_1^0} \quad (73)$$

where  $\gamma_1^\infty$  represents the infinite dilution activity coefficient of the primary solute in the adsorbed phase while  $q_2^0$  and  $C_1^0$  are from the single solute system of each solute at the same reduced spreading pressure. When  $\gamma_1^\infty$  is unit, we can define the IAST-predicted adsorbed amount as:

$$q_1^{IAST} = \frac{c_1 q_2^0}{c_1^0} \quad (74)$$

By substituting eq. 74 into eq. 72, we obtain

$$\gamma_1^\infty = \frac{q_1^{IAST}}{q_1} \quad (75)$$

eq. 75 not only provides a quick method to calculate  $\gamma_1^\infty$ , but also shows that  $\gamma_1^\infty$  directly compares  $q_1^{IAST}$  and the experimental adsorbed amount  $q_i$  under infinite dilution conditions.

### 3.2.2 Fitting Equations for Adsorbed Phase Activity Coefficients

$\gamma_i$  estimated using Wilson model is shown as follows

$$\ln \gamma_i = 1 - \ln\left(\sum_j^n z_j \Lambda_{ij}\right) - \sum_k^n \frac{z_k \Lambda_{ki}}{\sum_j^n z_j \Lambda_{kj}} \quad (76)$$

where  $z_j$  is the adsorbed phase fraction of component j.  $\Lambda_{ij}$  and  $\Lambda_{ji}$  are the adjustable parameters. For a binary solute mixture, the equations are expressed as

$$\ln \gamma_1 = 1 - \ln(z_1 + z_2 \Lambda_{12}) - \left(\frac{z_1}{z_1 + z_2 \Lambda_{12}}\right) - \left(\frac{z_2 \Lambda_{21}}{z_1 \Lambda_{21} + z_2}\right) \quad (77)$$

$$\ln \gamma_2 = 1 - \ln(z_2 + z_1 \Lambda_{21}) - \left(\frac{z_2}{z_2 + z_1 \Lambda_{21}}\right) - \left(\frac{z_1 \Lambda_{12}}{z_2 \Lambda_{12} + z_1}\right) \quad (78)$$

$\gamma_i$  estimated using NRTL model is shown below

$$\ln \gamma_i = \frac{\sum_j^n z_j \tau_{ji} G_{ji}}{\sum_k^n z_k G_{ki}} + \sum_j \left( \frac{z_j G_{ij}}{\sum_k^n z_k G_{kj}} \left( \tau_{ij} - \frac{\sum_k^n z_k \tau_{kj} G_{kj}}{\sum_k^n z_k G_{kj}} \right) \right) \quad (79)$$

with

$$G_{ji} = \exp(-\alpha_{ji}\tau_{ji}), \quad (80)$$

and

$$\tau_{ji} = \frac{g_{ji}-g_{ii}}{RT}, \quad \tau_{ii} = \tau_{jj} = 0 \quad (81)$$

$g_{ji}$  represents energy of interaction between component i and j.

For a binary solute mixture, NRTL equations are expressed as follows

$$\ln \gamma_1 = z_2^2 \left[ \tau_{21} \left( \frac{G_{21}}{z_1+z_2G_{21}} \right)^2 + \frac{\tau_{12}G_{12}}{(z_2+z_1G_{12})} \right] \quad (82)$$

$$\ln \gamma_2 = z_1^2 \left[ \tau_{21} \left( \frac{G_{12}}{z_2+z_1G_{12}} \right)^2 + \frac{\tau_{21}G_{21}}{(z_1+z_2G_{21})} \right] \quad (83)$$

with

$$G_{12} = \exp(-\alpha_{12}\tau_{12}), G_{21} = \exp(-\alpha_{12}\tau_{21}) \quad (84)$$

$\tau_{12}$ ,  $\tau_{21}$  and  $\alpha_{12}$  are three adjustable parameters for a binary solute mixture.

To obtain better fitting of  $\gamma_i^{exp}$ , we propose to use an empirical four-parameter model (FPM) shown as follows

$$\ln \gamma_1 = -A_1 z_2^{\beta_1} \quad (85)$$

$$\ln \gamma_2 = -A_2 z_1^{\beta_2} \quad (86)$$

where  $A_1$ ,  $A_2$ ,  $\beta_1$ , and  $\beta_2$  are adjustable parameters. The proposed FPM has been derived from the two-parameter Margules equation. In FPM, each  $\ln \gamma_i$  is allowed to have

different infinite values when  $z_j$  approaches zero, that is, each solute has its own  $A_i$ . In addition, each solute has its own adjustable exponent  $\beta_i$  to achieve better fitting.

All adjustable parameters in Wilson equation, NRTL model, and the FPM were calculated by performing least-square-error nonlinear regression on  $\gamma_i^{Exp}$ . Then, these models with fitting parameters determined based on experimental data were used to estimate  $\gamma_i$  for binary adsorption at other equilibrium conditions, results denoted as RAST. The process is described in **Figure 3**.

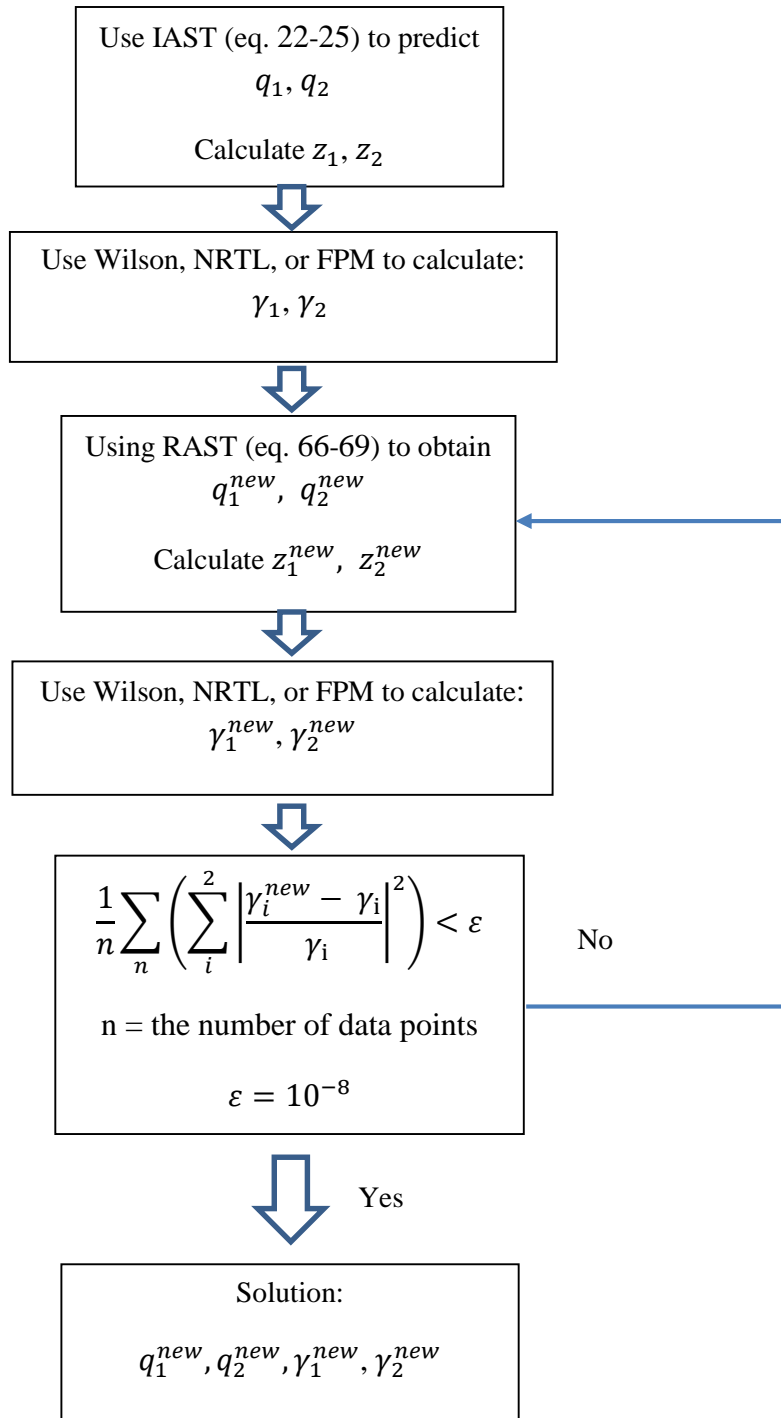


**Figure 3.** Procedure for iterative calculation of RAST  
with  $\gamma_i$  calculated based on fitting equations

### 3.3 Polyparameter Linear Free Energy Relationship (pp-LFER)

Abraham's pp-LFER has been widely used in the field of environmental science to study partitioning and sorption which has a general form for any specific partition ( $SP$ ):

$$SP = e\mathbf{E} + s\mathbf{S} + a\mathbf{A} + b\mathbf{B} + v\mathbf{V} + c \quad (87)$$

where  $SP$  is a physical chemical property of a solute related to Gibbs free energy of transfer between two phases of interests that can be either solvent such as water or a sorbed phase onto a sorbent such as NOM and AC. For instance,  $SP$  can be the logarithm of partitioning coefficient,  $\ln K_{w/ads}$ , of a known solute between water and the adsorbed phase onto an adsorbent. The terms  $\mathbf{E}$ ,  $\mathbf{S}$ ,  $\mathbf{A}$ ,  $\mathbf{B}$ , and  $\mathbf{V}$  stand for solute descriptors developed by Abraham's group.<sup>75</sup> The excess molar refraction ( $\mathbf{E}$ ) is used to capture nonspecific interactions associated with induced dipoles due to London dispersive forces and Debye forces;<sup>75</sup> the McGowan's characteristic volume ( $\mathbf{V}$ ) is intended to involve cavitation energy and some additional induced dipole-induced dipole forces;<sup>76</sup>  $\mathbf{S}$ , the polarity/polarizability parameter, is to account for permanent dipole involved interactions which partly overlap with  $\mathbf{E}$  for induced dipole forces; and  $\mathbf{A}$  and  $\mathbf{B}$  represent the overall H-bonding donating and accepting ability, respectively.<sup>77</sup> The counterparts of these solute descriptors,  $e$ ,  $s$ ,  $a$ ,  $b$ , and  $v$ , are coefficients determined by multiple linear regression analysis. They demonstrate the difference between the solution phase and, for example, the adsorbed phase, in their ability to participate in each interaction. It is worth noting that these coefficients can be dependent on the adsorbed amount when adsorption isotherm is nonlinear.<sup>78</sup>

In this project, we propose, for the first time, to study infinite adsorbed phase activity coefficients by pp-LFER. From eq. 72 we can derive

$$\ln \frac{c_1}{q_1} = \ln \frac{c_1^0}{q_2^0} + \ln \gamma_1^\infty \quad (88)$$

The left hand side can be treated as the partitioning coefficient,  $\ln K_{w/ads}(\Psi)$ , of the infinite dilute primary solute defined in **Section 3.2.1** between the aqueous phase and the adsorbed phase, which has been preloaded with a competitor with  $\Psi$ .  $\Psi$  is also the reduced spreading pressure of the bi-solute mixture system since the primary solute is infinite dilute.  $\ln K_{w/ads}(\Psi)$  thus can be expanded as

$$\begin{aligned} \ln K_{w/ads}(\Psi) = \ln \frac{c_1}{q_1} = & (e' + e(\Psi))\mathbf{E} + (s' + s(\Psi))\mathbf{S} + (a' + \\ & a(\Psi))\mathbf{A} + (b' + b(\Psi))\mathbf{B} + (v' + v(\Psi))\mathbf{V} + c' \end{aligned} \quad (89)$$

where the coefficients with primes are constants and the ones with brackets are a function of  $\Psi$ . The first term on the right hand side of eq. 88 is also a function of  $\Psi$ . Since it is related to single-solute isotherms, it can be expanded as

$$\begin{aligned} \ln \frac{c_1^0}{q_2^0} = & (e'' + e(\Psi))\mathbf{E} + (s'' + s(\Psi))\mathbf{S} + (a'' + a(\Psi))\mathbf{A} + (b'' + \\ & b(\Psi))\mathbf{B} + (v'' + v(\Psi))\mathbf{V} + c'' \end{aligned} \quad (90)$$

where the coefficients with two primes are constants and the ones with brackets are a function of  $\Psi$ . According to the previous assumptions in **Section 1.3**,  $\gamma_i^\infty$  is independent on  $\Psi$  and thus is the sole constant in eq. 88. Therefore, the  $\Psi$  dependent parts in eq. 89 and eq. 90 must cancel out, which will result in:

$$\ln \gamma_i^\infty = e\mathbf{E} + s\mathbf{S} + a\mathbf{A} + b\mathbf{B} + v\mathbf{V} + c \quad (91)$$

By keeping the same competitor while changing the primary solute, we can obtain a group of  $\gamma_i^\infty$  values, to which multiple linear regression can be applied to determine the coefficients in eq. 91. We will then be able to make prediction based on eq. 91 of the infinite activity coefficient of a solute with known solute descriptors.

## CHAPTER 4

### RESULTS AND DISCUSSION

#### 4.1 Single-Solute Adsorption

In **Figure 4**, the reduced spreading pressures calculated from Eq. 21 are plotted for all 8 compounds vs  $C_i^0$ . The ones with higher reduced spreading pressures are the more strongly adsorbed components. For a pair of two components, the strongly adsorbed component tends to be more stable in the adsorbed phase and the other one tends to be more stable in the aqueous phase.<sup>79</sup> Comparing **Figure 1** and **Figure 4**, we can find that the sequence of these compounds in an ascending order of adsorbed amount is the same as the one in an ascending order of reduced spreading pressure at the same equilibrium concentration, which is

$$\text{NB} > \text{4-CA} > \text{4-NA} > \text{4-CP} > \text{4-NP} > \text{4-MP} > \text{Aniline} > \text{Phenol}$$

The more strongly adsorbed component will likely be more competitive than a weakly adsorbed component. In a binary-solute adsorption system, the adsorbed amount of one solute will be reduced due to the presence of another solute. If we consider the condition of infinite dilute solution defined in **Section 3.2.1**, we can directly address the competitive effect of different solutes on a primary solute by comparing the adsorbed amounts of the primary solute based on IAST, that is,  $q_1^{IAST}$  in eq. 74. An example is given in **Figure 4** using 4-MP as the primary solute, 4-NA and Aniline as the competitors. We let the competitors, aniline and 4-NA, have the same concentration ( $C_2 \approx C_2^0 = 2$  mM, the vertical blue solid line in **Figure 4**).

Since the curves in **Figure 4** are plotted as  $\Psi$  vs.  $C_1^0$ ,  $\Psi$  of the mixtures 4-MP/aniline and 4-MP/4-NA can be found at the intersections of the vertical blue solid line with the curves of aniline and 4-NA respectively (assuming that infinite dilute 4-MP does not contribute to  $\Psi$  of the mixtures). To calculate  $q_1^{IAST}$  by eq. 74, we also need  $C_1^0$  values of 4-MP at the same spreading pressure. To obtain this value, we can draw a group of lines parallel to X axis at the respective  $\Psi$  value of aniline and 4-NA, the corresponding  $C_1^0$  values of 4-MP can be found at the intersections of the horizontal lines with the curve of 4-MP. According to eq. 74, a larger value of  $C_1^0$  results in a smaller

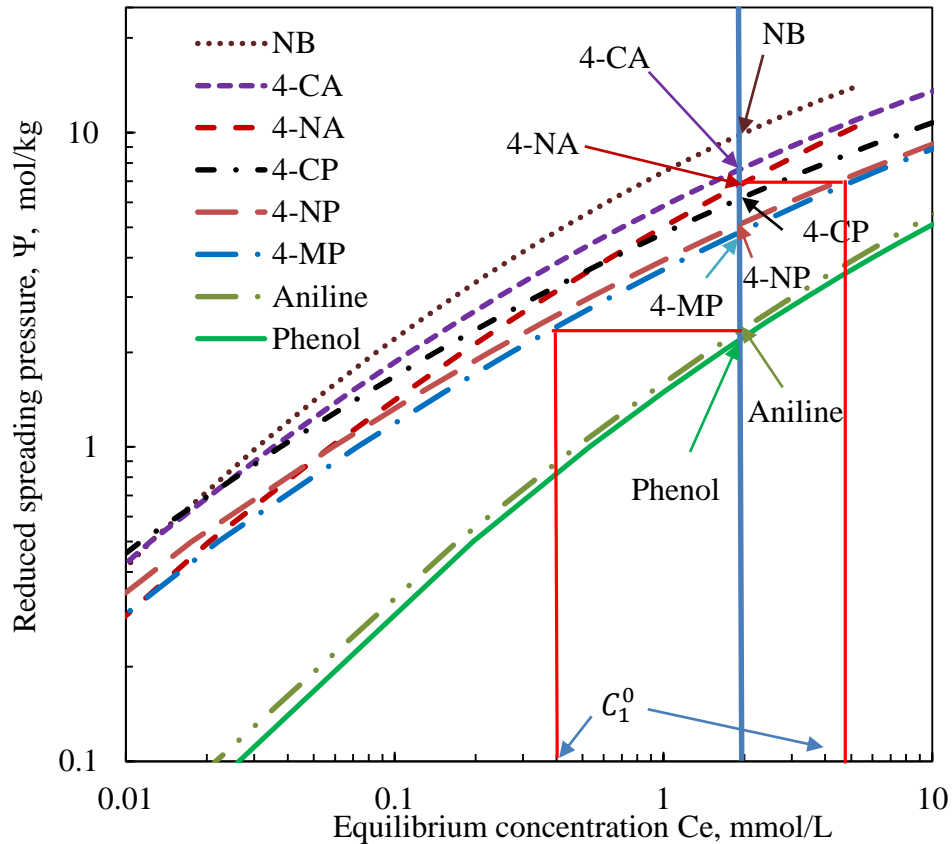


**Figure 4.** Calculated reduced spreading pressures of 8 aromatic compounds as single solutes as a function of equilibrium concentration

$q_1^{IAST}$  value, suggesting a stronger competitive effect of 4-NA (the difference in  $q_2^0$  is not considered since it is much smaller than that in  $C_1^0$ ). Therefore, 4-NA can reduce the adsorbed amount of 4-MP more than aniline. If the same method is applied to all solutes, the sequence of these solutes in ascending order of competitive effects is the same as the one shown above if IAST is valid. However, the sequence may be affected by nonideal behaviors of the primary solute in the presence of a competitor and altered by  $\gamma_1^\infty$ , as shown in Eq. 73 and discussed more extensively in **Section 4.3**.

## 4.2 Modeling Binary-Solute Adsorption

### 4.2.1 Comparison of IAST with SIAST and MSDSL

Binary adsorption data of 4-MP (primary solute) and aniline (competitor) is shown in **Table 4** and plotted in **Figure 5**. Data points in **Figure 5** from left to right correspond to an increasing amount of 4-MP. The equilibrium concentration of aniline decreased from 2.91 mmol/L to 2.62 mmol/L, which is about 10% as mentioned in **Section 3.1.8**. The adsorbed phase mole fraction  $z_i$  of each solute is reported for every other points, the range of which for the primary solute is about 0.014~0.923 from left to right in **Figure 5** (red arrow). Thus, the mole fraction of the competitor ranges correspondingly from 0.077 to 0.986 in the opposite direction (blue arrow). Single solute adsorption data of each solute is also plotted in comparison to bi-solute adsorption data. For either solute, it is shown that the adsorbed amount was reduced due to the competitive effect of the other solute, while binary adsorption isotherms approached those of the single solutes as their fractions approach unit. More competition arose with

decreasing adsorbed phase fraction as represented by the increasing deviation of the binary adsorption data from the single solute isotherms.

In **Figure 5**, as the concentration of 4-MP, the primary component, increases from the left to right hand, decreasing amounts of aniline are adsorbed onto MN200 due to the competition of 4-MP. When the mole fraction in the adsorbed phase decreases, left to right for aniline and the opposite direction for 4-MP, the adsorbed amounts predicted by all three models, i.e. IAST, SIAST, MSDSL, increasingly deviate from experimental adsorption equilibrium and become more underestimated. IAST tends to give better prediction of the more strongly adsorbed component, i.e. 4-MP, while SIAST and MSDSL perform better for the weakly adsorbed component, i.e. aniline.

As can be observed in **Figure 5**, none of the three predictive models, IAST, SIAST and MSDSL, could perfectly predict binary adsorption equilibrium for both the primary solute and the competitor at all mole fractions.

For binary pairs of 4-MP/ phenol, 4-MP/4-CP, and 4-NP/4-CP where ideal behavior in the adsorbed phase is expected due to similarity in their molecular structures, IAST performs much better than SIAST and MSDSLs as reflected by RMSE within 10% (**Table 5**). Although, for a few pairs with NB involved, SIAST is only slightly worse than IAST in general and even better in NB/4-CP system, we conclude the modeling of SIAST and MSDSL are worse than that of IAST. One explanation is that SIAST and MSDSL are both based on Langmuir types of isotherms. For aqueous phase adsorption onto microporous MN200, the adsorption mechanism is more likely pore-filling or multi-layer adsorption as oppose to single-layer adsorption (assumption of Langmuir equation).

**Table 4.** Binary adsorption equilibrium data with 4-MP as the primary solute and aniline as the competitor and model prediction based on IAST, SIAST, and MSDSL.

4-MP								aniline							
Exp. data		IAST		SIAST		MSDSL		Exp. data		IAST		SIAST		MSDSL	
C <sub>e</sub>	q <sub>e</sub>	q <sub>e</sub>	RE	q <sub>e</sub>	RE	q <sub>e</sub>	RE	C <sub>e</sub>	q <sub>e</sub>	q <sub>e</sub>	RE	q <sub>e</sub>	RE	q <sub>e</sub>	RE
mM	mmol	mmol/	%	mmol	%	mmol/	%	mM	mmol/	mmol	%	mmol/	%	mmol/	%
	/g	g		/g	g	g			g	/g		g	g	g	
0.011	0.043	0.028	35	0.026	41	0.014	67	2.91	1.65	1.56	5	1.53	7	1.54	7
0.021	0.061	0.053	14	0.048	22	0.027	56	2.90	1.60	1.54	4	1.52	6	1.53	5
0.034	0.13	0.084	35	0.077	41	0.044	66	2.84	1.63	1.50	8	1.48	9	1.51	8
0.060	0.20	0.14	27	0.13	33	0.077	61	2.85	1.52	1.46	4	1.45	4	1.49	2
0.10	0.29	0.22	24	0.21	29	0.12	59	2.81	1.48	1.40	6	1.40	5	1.46	2
0.23	0.52	0.45	13	0.43	17	0.26	49	2.88	1.33	1.26	5	1.31	2	1.41	6
0.38	0.70	0.66	5	0.63	10	0.41	41	2.90	1.22	1.13	7	1.21	1	1.35	11
0.50	0.86	0.80	7	0.75	12	0.52	40	2.82	1.19	1.03	13	1.13	5	1.28	8
0.84	1.10	1.08	2	1.00	8	0.76	31	2.84	1.07	0.88	18	1.03	3	1.18	11
1.60	1.45	1.50	3	1.37	5	1.17	19	2.78	0.88	0.67	23	0.89	1	1.00	15
2.97	1.88	1.93	3	1.79	5	1.66	12	2.82	0.78	0.51	34	0.76	2	0.83	7
5.07	2.26	2.31	2	2.21	2	2.14	5	2.86	0.67	0.39	41	0.64	4	0.67	0
8.22	2.62	2.67	2	2.62	0	2.59	1	2.72	0.57	0.28	50	0.50	13	0.49	14
11.56	2.78	2.91	5	2.89	4	2.88	3	2.71	0.47	0.23	50	0.42	11	0.39	16
18.45	3.07	3.23	5	3.21	5	3.23	5	2.66	0.38	0.17	55	0.31	18	0.28	27
25.84	3.24	3.44	6	3.41	5	3.43	6	2.62	0.33	0.14	58	0.25	24	0.21	36
33.39	3.48	3.60	3	3.54	2	3.56	2	2.62	0.29	0.12	61	0.21	29	0.17	43
RMSE			18	22		42					33	12		17	

Langmuir equation is thus not suitable for modeling adsorption isotherms in this study.

Another reason for the less accuracy of SIAST and MSDSL is that the adsorption energy distribution of adsorption sites on MN200 is more likely continuous. A segregated two-site model cannot precisely describe the heterogeneity of the solid surface.

In general, IAST always gives better prediction for the adsorption equilibrium of the strongly adsorbed component, that is, less error for 4-MP than aniline, 4-NP than 4-MP, 4-NA than aniline, and 4-CA than aniline etc., as reflected in **Table 5**.

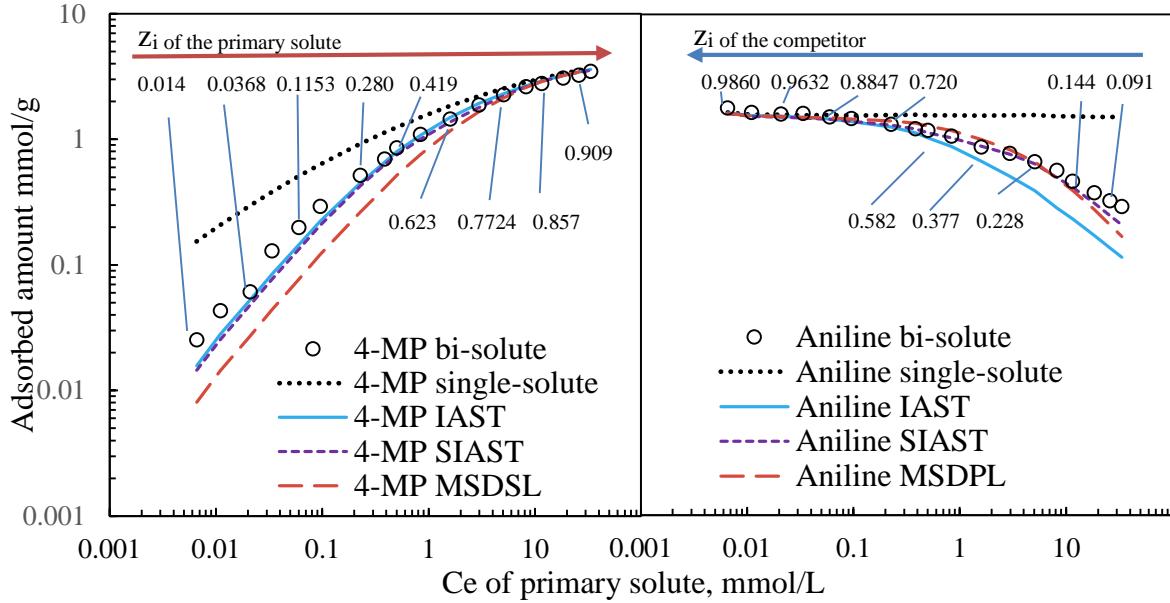


**Figure 5.** Binary adsorption of 4-MP (the primary solute) and aniline (the competitor).

#### 4.2.2 Comparison of RAST Incorporated with Wilson Equation, NRTL Model, and FPM

To correct for the deviation of IAST from experimental data,  $\gamma_i^{exp}$  was calculated for each component based on the method in **Section 3.2.1**. In Eqs. 66 and 67, if the  $\gamma_i$  values were calculated based on experimental data without fitting equations of activity coefficients, the results are denoted as RAST- $\gamma_i^{exp}$ . **Table 6** shows the errors of fitting  $q_1(C_1, C_2^{const})$ , the adsorbed amount of the primary solute in binary mixtures, as a function of its equilibrium concentration into the quadratic Freundlich equation, which is

necessary for using eq. 63. It can be seen that the quadratic Freundlich equation is able to describe well the adsorption isotherms of the primary solutes. As shown in **Figure 6**  $\gamma_i^{exp}$  can successfully eliminate the deviation of IAST with RMSE less than 8%. The good performance of RAST-  $\gamma_i^{exp}$  can be explained by two possible reasons. First, the  $\gamma_i^{exp}$  can be treated as independent on spreading pressure for solute-adsorbate equilibrium and thus Eq. 4 can be directly used in RAST instead of Eq. 7. Second, even if  $\gamma_i$  is dependent on spreading pressure, the last term in Eq. 7 is not significant for the adsorption on MN200, though it has a rigorous thermodynamic foundation.

**Table 5.** Summary of prediction results of IAST, SIAST and DSL

Adsorption Conditions				Root Mean Square Error of adsorbed amount %					
No.	Primary solute (P)	Competitor (C)	No. of batch	IAST		SIAST		DSL	
				P	C	P	C	P	C
1	4-MP	Phenol	16	5	8	12	82	34	95
2	4-MP	Aniline	17	18	33	22	12	42	17
3	4-MP	4-NP	16	13	8	23	37	39	68
4	4-MP	NB	18	12	10	18	18	27	15
5	4-MP	4-CA	9	30	23	41	10	51	13
6	4-MP	4-CP	20	7	6	21	20	10	13
7	4-MP	4-NA	14	5	7	9	33	43	43
8	Phenol	Aniline	18	18	34	21	33	15	42
9	Aniline	4-NA	16	28	5	38	16	41	6
10	Aniline	4-CA	12	26	5	33	7	26	6
11	NB	Aniline	12	13	21	15	24	20	17
12	NB	4-NA	14	6	4	6	9	18	16
13	NB	4-NP	14	24	28	23	25	26	16
14	NB	4-CA	14	24	19	38	15	40	17
15	NB	4-CP	14	23	25	20	4	13	23
16	4-NP	4-CP	16	4	8	9	15	42	45
17	4-CP	4-CA	16	14	17	13	12	39	25

The activity coefficients calculated above were then fitted into three models, Wilson equation, NRTL, and an empirical four-parameter model (FPM) (**Table 7**, and **Figure 7**). Generally, Wilson and NRTL have very similar fitting results while FPM fits the experimental activity coefficients better.

However, before we conclude that FPM is better than Wilson and NRTL models, we should test the ability of RAST combined with Wilson, NRTL, or FPM to predict adsorption equilibrium at different adsorption conditions. For this purpose, for each modeling set in **Table 5**, one additional set of new bi-solute adsorption data, switching the primary solute with the competitor, referred to as the test set hereafter, was collected and then compared to the predictions by RAST-NRTL, RAST-Wilson, and RAST-FPM using the parameters determined based on the previous data. At the same  $z_i$  of a solute, the modeling set and the corresponding test set have different total adsorption loadings and spreading pressures.

**Table 6.** Fitting results of the isotherms of primary solutes in binary mixtures and prediction results of  $q_e$  by RAST-  $\gamma_i^{exp}$

Adsorption Condition				RMSE of adsorbed amount (%)		
No. in <b>Table 5</b>	Primary solute	Competitor ( $C_{ini}$ )	No. of batch	Fitting results of $q_1(C_1, C_2^{const})$	Prediction of $q_e$ by RAST- $\gamma_i^{exp}$	
					primary	competitor
1	4-MP	Phenol (1mM)	16	/	/	/
2	4-MP	Aniline (1mM)	17	8	5	5
3	4-MP	4-NP (1mM)	16	3	3	3
4	4-MP	NB (1mM)	18	6	4	4
5	4-MP	4-CA (1mM)	9	9	3	3
6	4-MP	4-CP (1mM)	20	/	/	/
7	4-MP	4-NA (0.5mM)	14	/	/	/
8	Phenol	Aniline (1mM)	18	4	2	2
9	Aniline	4-NA (1mM)	16	10	8	8
10	Aniline	4-CA (0.5mM)	12	5	4	4
11	NB	Aniline (1.75mM)	12	5	4	6
12	NB	4-NA(1mM)	14	/	/	/
13	NB	4-NP(0.5mM)	14	3	2	2
14	NB	4-CA(0.5mM)	14	7	5	5
15	NB	4-CP(0.5mM)	14	3	2	2
16	4-NP	4-CP (1mM)	16	/	/	/
17	4-CP	4-CA(0.5mM)	14	4	4	4

Note: Binary adsorptions, No. 1, 6, 7, 12, and 16, are approximately ideal adsorbed mixtures since IAST predicts the adsorbed amounts with RMSEs less than 10% (**Table 5**) for both solutes. Thus, adsorbed phase activity coefficients were not calculated and RAST was not applied.

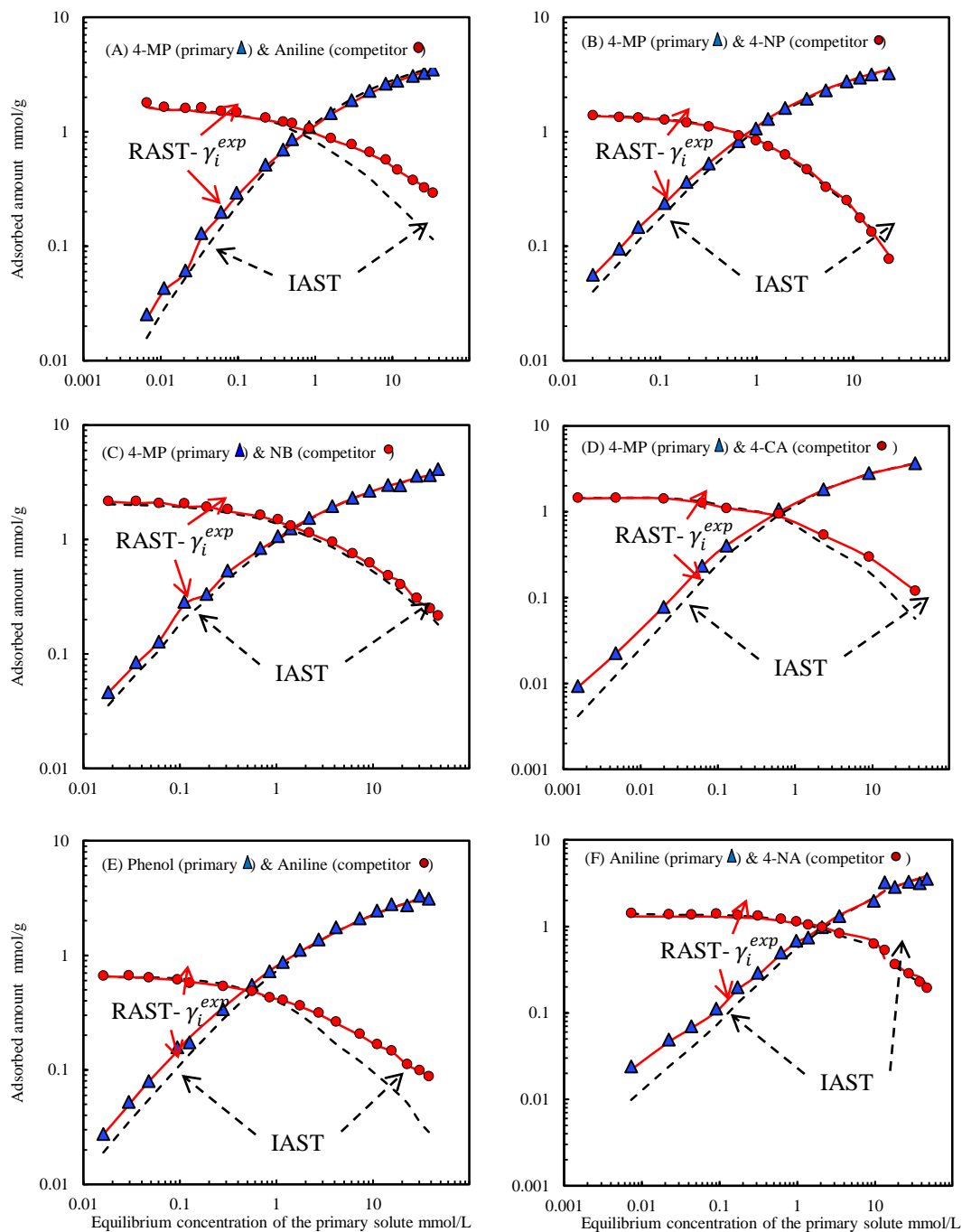


**Figure 6.** Plots of binary adsorption data in **Table 6** and prediction results by IAST and RAST- $\gamma_i^{exp}$

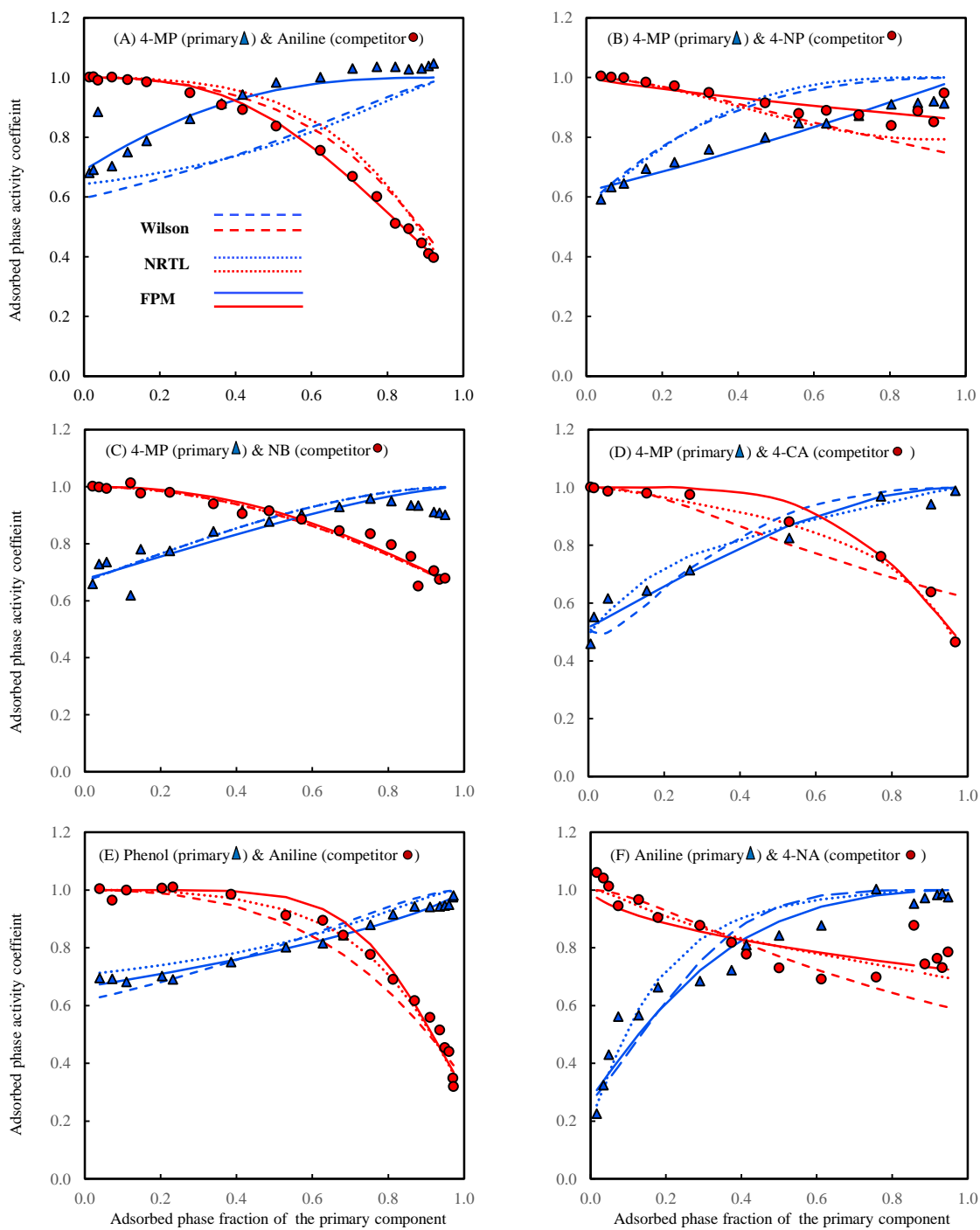


**Figure 7.** Experimental activity coefficients fitted

by Wilson, NRTL and FPM equations.

Predictions of the test sets by RAST with NRTL, Wilson and FPM are plotted in **Figure 8**, whose RMSEs are shown in **Table 8**. As reflected by smaller RMSEs, RAST-FPM performs better than RAST with Wilson or NRTL in most cases. RAST-FPM can reduce RMSEs to less than 10% when aniline was not involved. This suggests that (1) when  $\gamma_i^{exp}$  values are well fitted, RAST can accurately predict adsorbed amounts; (2) treating  $\gamma_i$  as independent on  $\Psi$  will not result in significant errors; and (3) binary adsorption systems with constant initial concentrations of the competitor, the method developed in this work, are better than those with constant ratios of initial concentrations used by Erto et al.<sup>8</sup> and Jadhav et al.<sup>21</sup> where varying concentration ratios of solutes were employed.

Nevertheless, when aniline was involved in the adsorbed mixture, the predicted adsorbed amount of aniline deviates significantly from the experimental data in the low concentration region as show in **Figure 8** (D) and (F), though activity coefficients were well fitted. Considering that the only difference between the modeling set and the test set is spreading pressure, we believe it is the spreading pressure dependency of  $\gamma_i$  that caused the less accurate prediction of RAST. This is most likely due to the heterogeneity of adsorption sites that is involved in the adsorption of aniline onto MN200. As discussed by Nguyen et al.<sup>80</sup> and Pan et al.,<sup>69</sup> the adsorbed aniline onto microporous sorbents resembles its pure liquid state at room temperature, and therefore, can access some occlusions inside the adsorbents that are not accessible to other solutes that are solids at room temperature (see their melting point in **Table 2**). As  $\Psi$  of the binary-solute adsorption system changes, the predicted  $q_1^{IAST}$  will change accordingly, but a part of the real adsorbed amount for aniline is not affected by competition. The overall result is that

$\gamma_i$  becomes dependent on  $\Psi$  for aniline. NB is also a liquid at room temperature as aniline, although with a higher melting point. The observation that its test sets were well predicted by RAST suggests that its  $\gamma_i$  is less likely dependent on  $\Psi$ . Future research is thus needed to elucidate the likely mechanism(s).

**Table 7.** Fitting results of  $\gamma_i$  by NRTL model, Wilson equation, and FPM

No. in <b>Table 5</b>	Adsorption Condition			RMSE of $\gamma_i$ (%)		
	Primary solute	Competitor	No. of Data Points	NRTL	Wilson	FPM
2	4-MP	Aniline	20	12	13	4
3	4-MP	4-NP	16	9	9	3
4	4-MP	NB	18	5	5	5
5	4-MP	4-CA	9	5	11	5
8	Phenol	Aniline	18	5	7	5
9	Aniline	4-NA	16	10	13	11
10	Aniline	4-CA	12	12	12	4
11	NB	Aniline	12	10	10	2
13	NB	4-NP	14	9	9	7
14	NB	4-CA	14	4	5	4
15	NB	4-CP	14	4	4	2
17	4-CP	4-CA	14	5	7	3

**Table 8.** Prediction of the test sets by RAST with NRTL model, Wilson equation, and FPM

Corresponding to <b>(Table 6)</b>	Adsorption Condition			RMSE of predicted $q_e$ (%)					
	Primary solute (P)	Competitor (C)	No. of Data Points	NRTL		Wilson		FPM	
				P	C	P	C	P	C
2	Aniline	4-MP	20	17	3	19	4	16	7
3	4-NP	4-MP	20	16	7	15	7	10	11
4	NB	4-MP	11	5	6	5	6	5	6
8	Aniline	Phenol	16	9	9	8	7	10	11
9	4-NA	Aniline	12	12	4	9	8	5	9
10	4-CA	Aniline	18	12	12	12	12	5	6
11	Aniline	NB	12	21	9	21	9	17	6
13	4-NP	NB	16	5	8	5	7	5	5
14	4-CA	NB	14	11	11	12	11	6	5
15	4-CP	NB	14	9	4	9	5	6	6

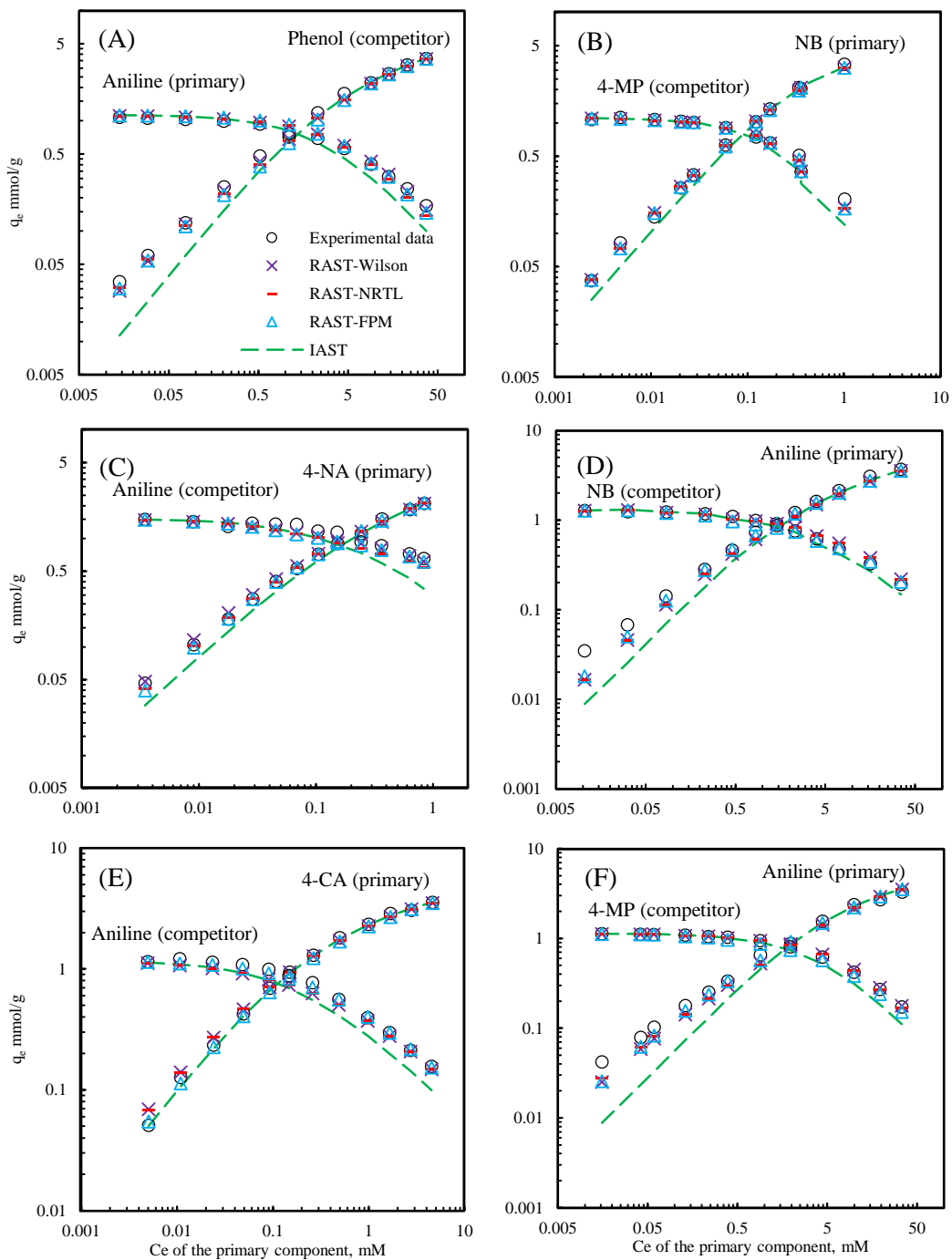


**Figure 8.** Comparison of experimental data of the test sets with prediction by RAST-Wilson, RAST-NRTL, RAST-FPM, and IAST

### 4.3 Adsorbate-Adsorbate Interactions and pp-LFER

Since the prediction of IAST for a solute increasingly deviates from experimental data as the mole fraction of the solute approaches zero, we extrapolated the nonideality to the infinite dilute condition to more conveniently discuss nonideality of the adsorbed mixtures.  $\gamma_i^\infty$  was calculated from NRTL, Wilson, and FPM models with the same parameters determined previously (letting  $z_i$  be zero) (**Table 9**). It is directly shown in Eq. 75 that an underestimated adsorbed amount by IAST will result in  $\gamma_i^\infty$  less than unit.

**Table 9.** Infinite dilution activity coefficients calculated from NRTL model, Wilson equation, and FPM by letting  $z_i$  be zero for each solute

	Solutes		$\gamma_i^\infty$					
	A	B	NRTL		Wilson		FPM	
			A	B	A	B	A	B
1	4-MP	Phenol	/	/	/	/	/	/
2	4-MP	Aniline	0.64	0.27	0.60	0.31	0.69	0.32
3	4-MP	4-NP	0.56	0.8	0.57	0.73	0.62	0.86
4	4-MP	NB	0.67	0.64	0.67	0.64	0.68	0.64
5	4-MP	4-CA	0.49	0.4	0.52	0.62	0.52	0.44
6	4-MP	4-CP	/	/	/	/	/	/
7	4-MP	4-NA	0.66	0.65	0.76	0.65	0.82	0.65
8	Phenol	Aniline	0.71	0.29	0.62	0.35	0.66	0.31
9	Aniline	4-NA	0.20	0.68	0.28	0.59	0.26	0.72
10	Aniline	4-CA	0.63	0.69	0.63	0.69	0.63	0.9
11	NB	Aniline	0.61	0.6	0.62	0.59	0.65	0.56
12	NB	4-NA	/	/	/	/	/	/
13	NB	4-NP	0.40	0.44	0.39	0.42	0.44	0.43
14	NB	4-CA	0.56	0.38	0.61	0.53	0.59	0.51
15	NB	4-CP	0.54	0.37	0.54	0.37	0.55	0.39
16	4-NP	4-CP	/	/	/	/	/	/
17	4-CP	4-CA	0.70	0.22	0.62	0.35	0.66	0.25

The smaller the  $\gamma_i^\infty$ , the more nonideal the solute is in the mixture. **Table 9** shows that all  $\gamma_i^\infty$  values are no larger than one for all solutes. This was noted as negative

deviation from Raoult's law and reported frequently in the literature for both gas phase adsorption and multi-solute adsorption.<sup>8, 20, 22, 48</sup> For solutes within the same chemical family, they tend to behave ideally in the adsorbed phase, for example, 4-MP/phenol, 4-MP/4-CP, and 4-NP/4-CP, though they have very different single-solute adsorption isotherms. However, for aniline/phenol, although they have very similar single-solute isotherms, their adsorbed phase mixture is nonideal. For aniline/4-MP, since the two solutes have very different single solute adsorption isotherms, they behave not surprisingly nonideally in the mixture. This is also true if we refer to other strongly nonideal mixtures such as 4-CP/4-CA and 4-MP/4-CA. These compounds are in solid states at room temperature so that the possible additional adsorption sites accessible to aniline are not available for them. Therefore, it strongly suggests that nonideality should not be interpreted solely based on the difference in single-solute isotherms or heterogeneity of the sorbent, but rather be attributed to possible intermolecular interactions among the adsorbed molecules.<sup>27</sup>

As shown in **Table 10**, the adsorbed mixtures of NB, a  $\pi$ -electron deficient solute, with either aniline or 4-MP, both  $\pi$ -electron sufficient solutes, are nonideal. To demonstrate whether  $\pi$ - $\pi$  EDA is the interaction causing the nonideality of the adsorbed mixtures, 4-NP and 4-NA, two  $\pi$ -electron deficient solutes, were mixed with NB. 4-NA and NB tend to form an ideal mixture in the adsorbed phase ( $\gamma_i^\infty = 0.9$ ) while nonideality is encountered in the 4-NP/NB mixture, as reflected by a  $\gamma_i^\infty$  of 0.43. Given the comparable **E** and **S** values for 4-NA and 4-NP (**Table 10**), 4-NA and 4-NP should be similar in terms of their ability to undergo  $\pi$ - $\pi$  EDA with NB. The observed different  $\gamma_i^\infty$  values are thus most likely associated with the strong H-bond donating ability of 4-NP

(large **A** value of 0.82 in **Table 10**). 4-NA is less likely to be involved in H-bonding (small **A** value of 0.42) with NB and thus behaves ideally in the adsorbed phase.

**Table 10.** Infinite dilution activity coefficients calculated based on FPM as shown in **Table 9** and solute Ambraham descriptors

Infinite dilute primary solute	competitor	$\gamma_i^\infty$ of the primary solute	solute descriptors of the primary solute <sup>69</sup>				
			E	S	A	B	V
Phenol	4-MP	0.90 <sup>b</sup>	0.81	0.89	0.6	0.3	0.775
Aniline	4-MP	0.32	0.96	0.96	0.26	0.41	0.816
4-CP	4-MP	0.90 <sup>b</sup>	0.92	1.08	0.67	0.2	0.898
4-NP	4-MP	0.86	1.07	1.72	0.82	0.26	0.949
4-NA	4-MP	0.65	1.22	1.91	0.42	0.38	0.991
4-CA	4-MP	0.44	1.06	1.13	0.3	0.31	0.939
NB	4-MP	0.64	0.87	1.11	0	0.28	0.891
(4-MP) <sup>a</sup>	4-MP	1.00 <sup>a</sup>	0.82	0.87	0.57	0.31	0.916
Phenol	NB	0.38	0.81	0.89	0.6	0.3	0.775
Aniline	NB	0.56	0.96	0.96	0.26	0.41	0.816
4-CP	NB	0.39	0.92	1.08	0.67	0.2	0.898
4-MP	NB	0.68	0.82	0.87	0.57	0.31	0.916
4-NP	NB	0.43	1.07	1.72	0.82	0.26	0.949
4-NA	NB	0.90 <sup>b</sup>	1.22	1.91	0.42	0.38	0.991
4-CA	NB	0.51	1.06	1.13	0.3	0.31	0.939
(NB) <sup>a</sup>	NB	1.00 <sup>a</sup>	0.87	1.11	0	0.28	0.891

Note: <sup>a</sup> Hypothetical primary solute, which means that the primary solute and the competitor are the same compound and thus the binary systems are perfectly ideal. <sup>b</sup>  $\gamma_i^\infty$  is assume to be 0.90 for approximately ideal adsorbed mixtures as shown in **Table 6** that can be predicted by IAST with RMSE less than 10% and were thus not further predicted by RAST.

For the purpose of quantitatively predicting nonideality of adsorbed mixtures, pp-LFER was applied to correlating  $\gamma_i^\infty$  with physical-chemical properties of the solutes, i.e. the solute descriptors in **Table 10**. Two binary-solute series were chosen: varying infinite

dilute primary solutes with either 4-MP or NB as the fixed competitor. By multiple linear regression, the best obtained regressions based on the lowest Mallow's Cp values are:

$$\ln \gamma_i^{\infty,4-MP} = (-4.166 \pm 1.217)\mathbf{E} + (0.923 \pm 0.4671)\mathbf{S} + (0.7018 \pm 0.3169)\mathbf{A} + (2.686 \pm 1.646)\mathbf{V} - 0.22 \quad (R_{adj}^2 = 0.741) \quad (92)$$

$$\ln \gamma_i^{\infty,NB} = (-3.322 \pm 1.101)\mathbf{E} + (0.8507 \pm 0.3839)\mathbf{S} + (-0.9699 \pm 0.2778)\mathbf{A} + (2.997 \pm 1.253)\mathbf{B} + (4.007 \pm 1.890)\mathbf{V} - 2.45 \quad (R_{adj}^2 = 0.812) \quad (93)$$

Since  $\gamma_i^{\infty}$  is less than unit, and correspondingly  $\ln \gamma_i^{\infty}$  is negative for nonideal behavior of an adsorbate, the negative product of one solute descriptor with its coefficient in eqs. 92 and 93 means the term will increase nonideality as an additional interaction. For the series with 4-MP as the fixed competitor (eq. 92), the best regression was obtained with  $\mathbf{E}$ ,  $\mathbf{S}$ ,  $\mathbf{A}$ , and  $\mathbf{V}$ . It seems that H-bonding accepting ability  $\mathbf{A}$  is not statistically significant.  $\mathbf{E}$  is the only descriptor with a negative coefficient, which implies the nonideality is more related to induced-dipole related interactions. For the series with NB as the fixed competitor (eq. 93), all solute descriptors are involved while both  $\mathbf{E}$  and  $\mathbf{A}$  contribute to the nonideality. From the point view of thermodynamics,  $\ln \gamma_i$  is related to partial molar excess Gibbs free energy. Thus, eq. 91 can also be viewed as a regression on excess Gibbs free energy. The application of pp-LFER in this work can be viewed as an empirical rather than theoretical approach. A more rigorous interpretation with a much larger number of compounds involved in developing pp-LFERs is warranted for a thorough understanding of the interaction forces contributing to the nonideality of adsorbed mixtures.

The calculated  $\gamma_i^\infty$  values based on eq. 92 and eq. 93 are plotted in **Figure 9** vs. exp.  $\gamma_i^\infty$ . The good regression results as reflected by  $R_{adj}^2$  and in **Figure 9** suggest that pp-LFER is a promising method to predict adsorbed phase activity coefficients, although the linear relationships were developed involving only 8 compounds in this work and are not robust enough yet. To the best of our knowledge, this is the first time that pp-LFER was applied to interpreting and predicting adsorbed phase activity coefficients.

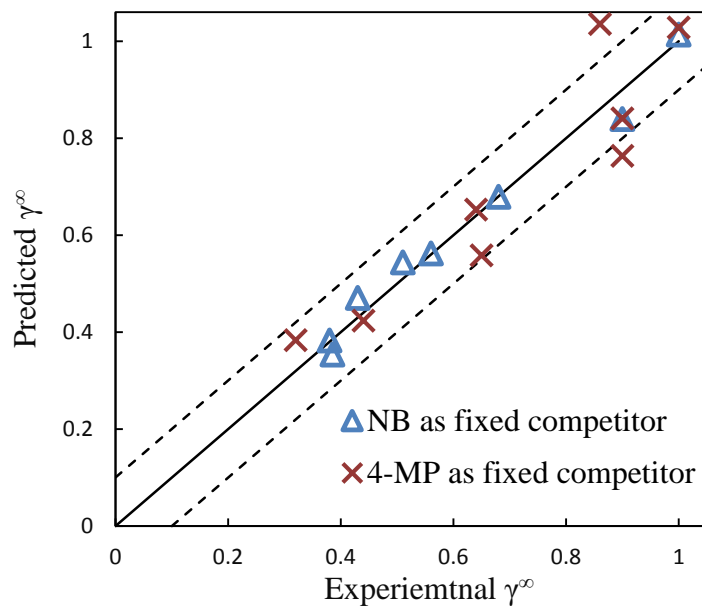


**Figure 9.** Compare calculated  $\gamma_i^\infty$  based on linear relationships with  $\gamma_i^\infty$  obtained experimentally. The dashed lines represent 10% errors of  $\gamma_i^\infty$  prediction which will result in about 9~11% error in the predicted adsorbed amount according to Eq. 73

The  $\gamma_i^\infty$  values of the primary solutes, once obtained from the linear relationships, can be used to calculate the parameters in activity coefficient models. For Wilson equation (eqs. 77 and 78), it was assumed that  $\gamma_2^\infty$  of the competitor is the same as  $\gamma_1^\infty$  of

the primary solute and then the two parameters,  $\Lambda_{12}$  and  $\Lambda_{21}$ , can be calculated from eqs. 94 and 95 which were derived from eq. 77 and 78 by letting either  $z_1$  or  $z_2$  be zero.

$$\ln \gamma_1^\infty = 1 - \ln \Lambda_{12} - \Lambda_{21} \quad (94)$$

$$\ln \gamma_2^\infty = 1 - \ln \Lambda_{21} - \Lambda_{12} \quad (95)$$

By incorporating the values of  $\Lambda_{12}$  and  $\Lambda_{21}$  into eqs. 77 and 78, RAST-Wilson can be applied to estimating bi-solute adsorption capacities.

For FPM (eqs. 85-86), we proposed to treat  $\beta_1$  and  $\beta_2$  as 2 as the original Margules equations while letting  $A_1$  be  $(-\ln \gamma_1^\infty)$  for the primary solute ( $z_2=1$  in eq 85) and  $A_2$  be zero for the competitor (assuming ideal behavior for the competitor since  $z_1$  is close to 0 in eq. 86).

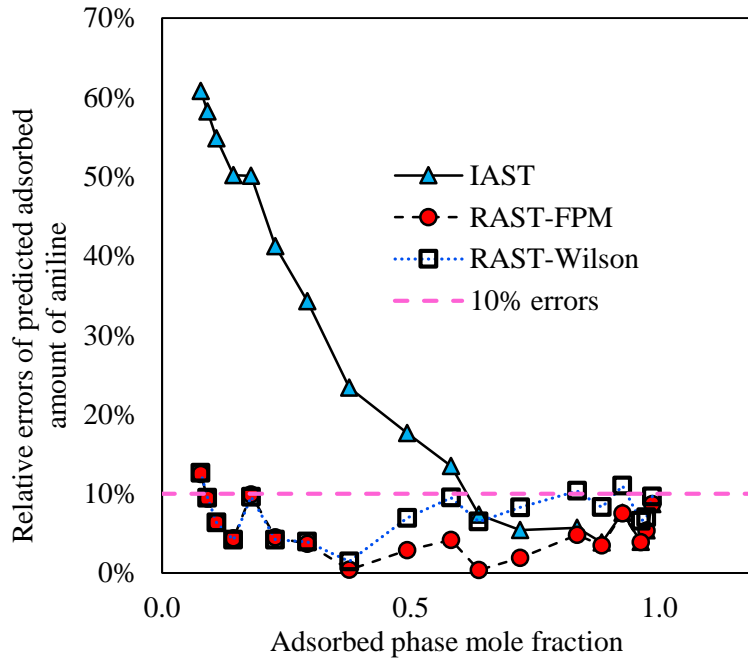


**Figure 10.** Prediction errors of the adsorbed amounts of aniline in the presence of 4-MP (test set) using  $\gamma_i$  extrapolated from  $\gamma_i^\infty$ .

By changing the  $z_i$  values, the non-infinite activity coefficients at different mole fractions were then calculated and incorporated in RAST by implementing the iteration process shown in **Figure 3**. As shown in **Figure 10**, errors for the predicted amount of aniline adsorbed in the presence of 4-MP, based on either RAST-Wilson or RAST-FPM, were generally less than 10% for all fractions of aniline. Much larger errors, particularly at lower mole fractions, are observed when only IAST was applied for the prediction purposes.

#### **4.4 Tri- and Tetra-Solute Adsorption of Aniline, Phenol, and 4-MP in the Presence of a High Concentration of Nitrobenzene**

As shown in **Figure 11a**, the adsorption isotherm of aniline in the presence of a large amount of NB (aniline @ NB) overlaps with its adsorption isotherms when an equal amount of phenol or 4-MP was also in present. Even for the tetra-solute mixture containing an equal amount of aniline, phenol, and 4-MP and a large amount of NB, the adsorption isotherm of aniline is unaffected. This demonstrates that in the presence of a dominant contaminant such as NB, the competitive effects on aniline have come solely from NB, and there is negligible interaction among the dilute solutes. Similar behaviors of 4-MP were observed in the same adsorption systems as mentioned above (**Figure 11b**), i.e., the adsorption isotherms of 4-MP in the bi-, tri-, and tetra-solute adsorption systems overlap with each other which indicates negligible interactions among the dilute solutes.

The adsorbed amounts of NB are close to the values predicted by IAST and are not shown here (around 2.45 mmol/g). The adsorbed phase mole fraction of aniline or 4-

MP is from 0.01 to 0.1 from the left to right. The predicted adsorbed amounts of aniline based on RAST-FPM obviously deviate from the experimental data while the prediction for 4-MP by RAST-FRP agrees with the experimental data for all mixtures. As the fraction of aniline decreases, the error in its predicted adsorbed amounts increases. The calculated  $\gamma_i$  for aniline based on eq. 75 approaches zero as  $z_i$  keeps decreasing, which cannot be described by any known activity coefficient models. This means that our proposed method has its limitation in the extremely small  $z_i$  value region for aniline. This might be associated with the same reason as discussed on page 42. For all other solutes, just like 4-MP, because of the accurate modeling for bi-solute mixtures, similar small errors are expected when predicting their adsorbed amounts in tri- and tetra-solute mixtures.

Although the fundamental mechanism of nonideality is still not fully addressed, our tri- and tetra-solute adsorption data showed that the predominating solute, NB in this case, solely contributed to the competitive effect while the dilutes solutes tend not to interact with each other. This indicates that for each solute, the competitive effects can be independently considered and a multi-component system with  $n$  components but only one component dominating can be treated as  $(n-1)$  bi-solute systems separately. This will significantly simplify the calculation for modeling multi-component adsorption while it is also close to many real systems where there is one major contaminant or a large amount of NOM in present.

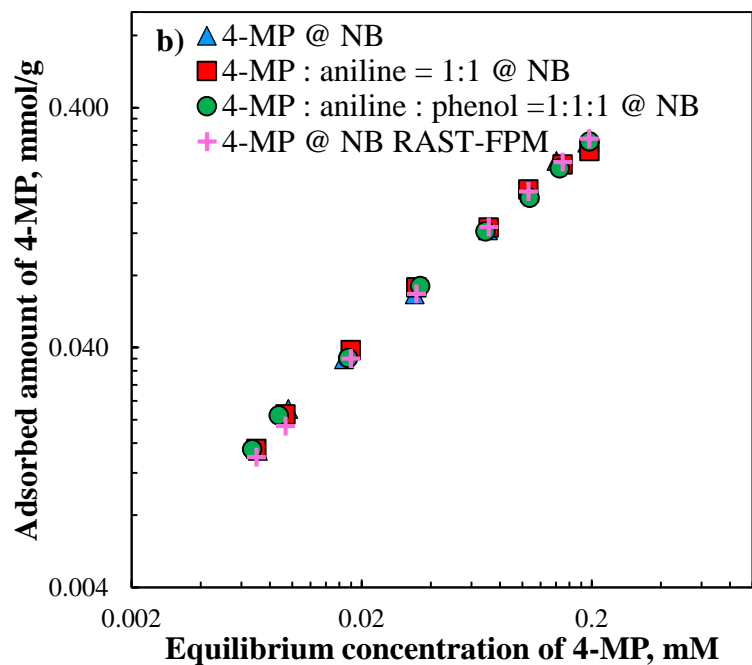
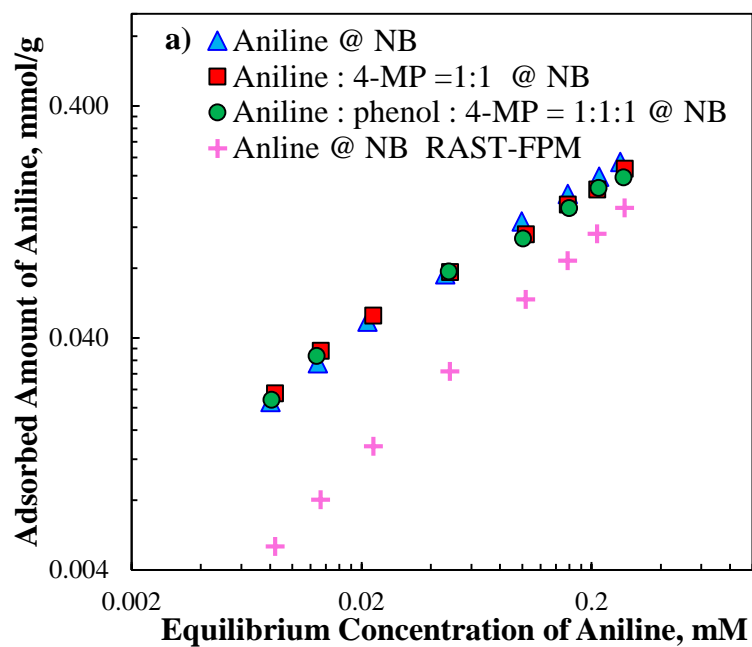


**Figure 11.** Tri- and tetra-solute adsorption of aniline, phenol, and 4-MP in the presence of a high concentration of nitrobenzene  $\sim 0.45$  mM.

## CHAPTER 5

### CONCLUSIONS

In this project, we applied three predictive models, namely IAST, SIAST and MSDSL, and an empirical model, RAST, to studying binary-solute adsorption of NB, aniline, 4-CA, 4-NA, phenol, 4-MP, 4-NP, and 4-CP onto MN200. Results show that IAST incorporated with an empirical quadratic Freundlich equation is better than SIAST and MSDSL, both of which rely on the dual-site Langmuir model. To improve the accuracy of IAST prediction, adsorbed phase activity coefficients were calculated based on experimental data. Three methods of designing binary-solute batch experiments and calculating  $\gamma_i$  (and also  $\gamma_i^\infty$ ) were developed and provided in detail. Our work shows that  $\gamma_i$  can be treated as spreading-pressure independent. The better fitting of FPM, proposed in the present work, than Wilson and NRTL models can improve the accuracy of RAST prediction. The nonideality of different binary-solute mixtures in the adsorbed phase was compared based on  $\gamma_i$ . Adsorbate-adsorbate interactions are likely involved.

When correlating  $\gamma_i^\infty$  with solute descriptors based on pp-LFERs, two empirical linear relationships were developed for adsorption of infinite dilute solutes in the presence of two major contaminants, 4-MP and NB, respectively. Results show that pp-LFER has a great potential in predicting  $\gamma_i^\infty$ , which can be extrapolated to non-infinite conditions by Wilson equation and FPM with a few assumptions. Overall, our results have moved a major step forward in accurately simulating and predicting bi-solute adsorption based on single-solute adsorption isotherms.

Since accurate equilibrium adsorption data is desirable in predicting breakthrough curves for fixed-bed column adsorption,<sup>10</sup> the efforts of this work is important for the application of column adsorption models in real systems. The bi-solute adsorption experiments in this work have covered a wide range of concentrations of simple aromatic compounds and concentration ratios. They were successfully simulated while test sets were accurately predicted. The infinite condition defined in this work, which has one predominating solute with a high concentration, is very common in real wastewater streams, for example, from a coking plant.<sup>81</sup> Although our tri- and tetra- solute adsorption experiments showed some limitation when the aniline had extremely low mole fraction, the proposed method of treating  $n$ -component systems as  $n$  independent bi-solute systems is promising in studying mixtures with multiple components. Furthermore, this approach has a great potential in studying the competitive effects of the predominating NOM in water systems if we treat the NOM as the major competitor.

## **CHAPTER 6**

### **FUTURE WORK**

For future application, the pp-LFER approach should be further tested with a large number of solutes with diverse structures, especially from different chemical families. A more rigorous interpretation as well as more direct evidence is in need for the relationships between adsorbate-adsorbate interactions and nonideality of the adsorbed mixtures. Another limitation of our developed approach is that the competitor has to be the same for one series of compounds. This condition may be encountered in wastewaters where one particular pollutant dominates while other targeted contaminants can be treated as infinite dilute. This is especially the case when dissolved organic matter is the dominant component in the water while the concentrations of all contaminants are much lower. Therefore, studies should be carried out to develop models for such water treatment. Finally, future work should also be carried out to apply the developed approaches to adsorption systems with more than four solutes.

## REFERENCES CITED

1. Abrams, D. S.; Prausnitz, J. M., Statistical thermodynamics of liquid-mixtures - new expression for excess gibbs energy of partly or completely miscible systems. *AIChE J* **1975**, *21*, (1), 116-128.
2. Benotti, M. J.; Trenholm, R. A.; Vanderford, B. J.; Holady, J. C.; Stanford, B. D.; Snyder, S. A., Pharmaceuticals and endocrine disrupting compounds in U.S. drinking water. *Environ. Toxicol. Chem.* **2009**, *43*, 597–603.
3. Calleja, G.; Jimenez, A.; Pau, J.; Dominguez, L.; Perez, P., Multicomponent adsorption equilibrium of ethylene, propane, propylene and CO<sub>2</sub> on 13x-zeolite. *Gas Sep. Purif.* **1994**, *8*, (4), 247-256.
4. Ceresi, J. E. J.; Tien, C., Carbon adsorption of phenol from aqueous solutions in the presence of other adsorbates. *Sep. Technol.* **1991**, *1*, (5), 273–281.
5. McMurry, L. M.; Oethinger, M.; Levy, S. B., Triclosan targets lipid synthesis. *Nature* **1998**, *394*, (6693), 531-532.
6. EPA, U. <http://water.epa.gov/scitech/methods/cwa/pollutants.cfm>
7. McKenna, M., The enemy within: A new pattern of antibiotic resistance. *Scientific American* 2011, p 12.
8. Erto, A.; Lancia, A.; Musmarra, D., A real adsorbed solution theory model for competitive multicomponent liquid adsorption onto granular activated carbon. *Micropor. Mesopor. Mat.* **2012**, *154*, 45-50.
9. Valderrama, C. s.; Poch, J.; Barios, J. I.; Farran, A.; Cortina, J. L., Binary fixed bed modeling of phenol/aniline removal from aqueous solutions onto hyper-cross-linked resin (Macronet MN200). *J. Chem. Eng. Data* **2012**, *57*, (5), 1502-1508.
10. Xu, Z.; Cai, J.-g.; Pan, B.-c., Mathematically modeling fixed-bed adsorption in aqueous systems. *J. Zhejiang Univ. Sci. A* **2013**, *14*, (3), 155-176.
11. Myers, A. L.; Prausnitz, J. M., Thermodynamics of mixed-gas adsorption. *AIChE J.* **1965**, *11*, 121-127.

12. Radke, C. J.; Prausnitz, J. M., Thermodynamics of multi-solute adsorption from dilute liquid solutions. *AIChE J* **1972**, *18*, (4), 761-768.
13. Costa, E.; Sotelo, J. L.; Calleja, G.; Marron, C., Adsorption of binary and ternary hydrocarbon-gas mixtures on activated carbon - Experimental-determination and theoretical prediction of the ternary equilibrium data. *AIChE J* **1981**, *27*, (1), 5-12.
14. Talu, O.; Zwiebel, I., Multicomponent adsorption equilibria of nonideal mixtures. *AIChE J.* **1986**, *32*, (8), 1263-1276.
15. Sakuth, M.; Meyer, J.; Gmehling, J., Measurement and prediction of binary adsorption equilibria of vapors on dealuminated Y-zeolites (DAY). *Chem Eng Process* **1998**, *37*, (4), 267-277.
16. Myers, A. L., Prediction of adsorption of nonideal mixtures in nanoporous materials. *Adsorption* **2005**, *11*, 37-42.
17. Valenzuela, D. P.; Myers, A. L.; Talu, O.; Zwiebel, I., Adsorption of gas-mixtures - effect of energetic heterogeneity. *AIChE J* **1988**, *34*, (3), 397-402.
18. Swisher, J. A.; Lin, L. C.; Kim, J.; Smit, B., Evaluating mixture adsorption models using molecular simulation. *AIChE J.* **2013**, *59*, (8), 3054-3064.
19. Ritter, J. A.; Bhadra, S. J.; Ebner, A. D., On the use of the dual-process Langmuir model for correlating unary equilibria and predicting mixed-gas adsorption equilibria. *Langmuir* **2011**, *27*, (8), 4700-4712.
20. Myers, A. L., Activity-coefficients of mixtures adsorbed on heterogeneous surfaces. *AIChE J* **1983**, *29*, (4), 691-693.
21. Jadhav, A. J.; Srivastava, V. C., Adsorbed solution theory based modeling of binary adsorption of nitrobenzene, aniline and phenol onto granulated activated carbon. *Chem Eng J* **2013**, *229*, 450-459.
22. Erto, A.; Lancia, A.; Musmarra, D., A modelling analysis of PCE/TCE mixture adsorption based on Ideal Adsorbed Solution Theory. *Sep. Purif. Technol.* **2011**, *80*, (1), 140-147.

23. Zhu, D.; Pignatello, J. J., A concentration-dependent multi-term linear free energy relationship for sorption of organic compounds to soils based on the hexadecane dilute-solution reference state. *Environ. Sci. Technol.* **2005**, *39*, (22), 8817-8828.
24. Crittenden, J. C.; Luft, P.; Hand, D. W.; Oravltz, J. L.; Loper, S. W.; Arit, M., Prediction of multicomponent adsorption equilibria using ideal adsorbed solution theory. *Environ. Sci. Technol.* **1985**, *19*, 1037-1043.
25. Xing, B.; Pignatello, J. J., Competitive sorption between 1, 3-dichlorobenzene or 2, 4-dichlorophenol and natural aromatic acids in soil organic matter. *Environ. Sci. Technol.* **1998**, *32*, (5), 614-619.
26. Yang, K.; Wang, X.; Zhu, L.; Xing, B., Competitive sorption of pyrene, phenanthrene, and naphthalene on multiwalled carbon nanotubes. *Environ. Sci. Technol.* **2006**, *40*, (18), 5804-5810.
27. Zhang, W.; Xu, Z.; Pan, B.; Zhang, Q.; Du, W.; Zhang, Q.; Zheng, K.; Zhang, Q.; Chen, J., Adsorption enhancement of laterally interacting phenol/aniline mixtures onto nonpolar adsorbents. *Chemosphere* **2007**, *66*, (11), 2044-2049.
28. Yang, K.; Wu, W.; Jing, Q.; Jiang, W.; Xing, B., Competitive adsorption of naphthalene with 2, 4-dichlorophenol and 4-chloroaniline on multiwalled carbon nanotubes. *Environ. Sci. Technol.* **2010**, *44*, (8), 3021-3027.
29. Chen, H. B.; Sholl, D. S., Examining the accuracy of ideal adsorbed solution theory without curve-fitting using transition matrix Monte Carlo simulations. *Langmuir* **2007**, *23*, (11), 6431-6437.
30. Choy, K. K. H.; Porter, J. F.; McKay, G., Single and multicomponent equilibrium studies for the adsorption of acidic dyes on carbon from effluents. *Langmuir* **2004**, *20*, (22), 9646-9656.
31. Richter, E.; Schutz, W.; Myers, A. L., Effect of adsorption equation on prediction of multicomponent adsorption equilibria by the Ideal Adsorbed Solution Theory. *Chem Eng Sci* **1989**, *44*, (8), 1609-1616.

32. Hu, X. J.; Do, D. D., Comparing various multicomponent adsorption equilibrium-models. *AIChE J* **1995**, *41*, (6), 1585-1592.
33. Fritz, W.; Schlunder, E., Competitive adsorption of two dissolved organics onto activated carbon. Pt. 1: adsorption equilibria. *Chem Eng Sci* **1981**, *36*, (4), 721-30.
34. Jossens, L.; Prausnitz, J. M.; Fritz, W.; Schlunder, E. U.; Myers, A. L., Thermodynamics of multi-Solute adsorption from dilute aqueous-solutions. *Chem Eng Sci* **1978**, *33*, (8), 1097-1106.
35. Porter, J. F.; McKay, G.; Choy, K. H., The prediction of sorption from a binary mixture of acidic dyes using single- and mixed-isotherm variants of the ideal adsorbed solute theory. *Chem Eng Sci* **1999**, *54*, (24), 5863-5885.
36. Smith, E. H., Evaluation of multicomponent adsorption equilibria for organic mixtures onto activated carbon. *Water Res* **1991**, *25*, (2), 125-134.
37. Thacker, W. E.; Crittenden, J. C.; Snoeyink, V. L., Modeling of adsorber performance - variable influent concentration and comparison of adsorbents. *J Water Pollut Con F* **1984**, *56*, (3), 243-250.
38. Xing, B.; Pignatello, J. J.; Gigliotti, B., Competitive sorption between atrazine and other organic compounds in soils and model sorbents. *Environ. Sci. Technol.* **1996**, *30*, 2432-2440.
39. Crittenden, J. C.; Luft, P.; Hand, D. W., Prediction of multicomponent adsorption equilibria in background mixtures of unknown composition. *Water Res* **1985**, *19*, (12), 1537-1548.
40. Najm, I. N.; Snoeyink, V. L.; Richard, Y., Effect of initial concentration of a SOC in natural water on its adsorption by activated carbon. *J.-Am. Water Works Assoc.* **1991**, 57-63.
41. Graham, M.; Summers, R.; Simpson, M.; MacLeod, B., Modeling equilibrium adsorption of 2-methylisoborneol and geosmin in natural waters. *Water Res* **2000**, *34*, (8), 2291-2300.

42. Zietzschmann, F.; Worch, E.; Altmann, J.; Ruhl, A. S.; Sperlich, A.; Meinel, F.; Jekel, M., Impact of EfOM size on competition in activated carbon adsorption of organic micro-pollutants from treated wastewater. *Water Res* **2014**, *65*, 297-306.
43. Talu, O.; Myers, A. L., Rigorous thermodynamic treatment of gas adsorption. *AIChE J.* **1988**, *34*, (11), 1887-1893.
44. Sochard, S.; Fernandes, N.; Reneaume, J. M., Modeling of adsorption isotherm of a binary mixture with real adsorbed solution theory and nonrandom two-liquid model. *AIChE J* **2010**, *56*, (12), 3109-3119.
45. Garcia-Galdo, J. E.; Cobas-Rodriguez, J.; Jáuregui-Haza, U. J.; Guiochon, G., Improved model of multicomponent adsorption in reversed-phase liquid chromatography. *J. Chromatogr. A* **2004**, *1024*, (1), 9-14.
46. Furmaniak, S.; Koter, S.; Terzyk, A. P.; Gauden, P. A.; Kowalczyk, P.; Rychlicki, G., New insights into the ideal adsorbed solution theory. *Phys. Chem. Chem. Phys.* **2015**, *17*, (11), 7232-7247.
47. Ushiki, I.; Ota, M.; Sato, Y.; Inomata, H., Prediction of VOCs adsorption equilibria on activated carbon in supercritical carbon dioxide over a wide range of temperature and pressure by using pure component adsorption data: Combined approach of the Dubinin-Astakhov equation and the non-ideal adsorbed solution theory (NIAST). *Fluid Phase Equilib.* **2014**, *375*, 293-305.
48. Talu, O.; Li, J.; Myers, A. L., Activity coefficients of adsorbed mixtures. *Adsorption* **1995**, *1*, (2), 103-112.
49. Siperstein, F. R.; Myers, A. L., Mixed-gas adsorption. *AIChE J.* **2001**, *47*, 1141-1159
50. Mota, J. P. B.; Rodrigo, A. J. S., Calculations of multicomponent adsorption-column dynamics combining the potential and ideal adsorbed solution theories. *Ind Eng Chem Res* **2000**, *39*, (7), 2459-2467.
51. Zhang, W.; Zhang, Q.; Pan, B.; Lv, L.; Pan, B.; Xu, Z.; Zhang, Q.; Zhao, X.; Du, W.; Zhang, Q., Modeling synergistic adsorption of phenol/aniline mixtures in the

- aqueous phase onto porous polymer adsorbents. *J. Colloid Interface Sci.* **2007**, *306*, (2), 216-221.
52. Valderrama, C.; Barrios, J. I.; Farran, A.; Cortina, J. L., Evaluating binary sorption of phenol/aniline from aqueous solutions onto granular activated carbon and hypercrosslinked polymeric resin (MN200). *Water Air Soil Pollut.* **2010**, *210*, (1-4), 421-434.
53. Sander, M.; Pignatello, J. J., Characterization of charcoal adsorption sites for aromatic compounds: insights drawn from single-solute and bi-solute competitive experiments. *Environ. Sci. Technol.* **2005**, *39*, (6), 1606-1615.
54. Abburi, K., Adsorption of phenol and p-chlorophenol from their single and bisolute aqueous solutions on Amberlite XAD-16 resin. *J. Hazard. Mater.* **2003**, *105*, (1), 143-156.
55. Sulaymon, A. H.; Ahmed, K. W., Competitive adsorption of furfural and phenolic compounds onto activated carbon in fixed bed column. *Environmental science & technology* **2007**, *42*, (2), 392-397.
56. Valderrama, C.; Barrios, J. I.; Farran, A.; Cortina, J. L., Evaluation of phenol/aniline (single and binary) removal from aqueous solutions onto hyper-cross-linked polymeric resin (Macronet MN200) and granular activated carbon in fixed-bed column. *Water, Air, & Soil Pollution* **2011**, *215*, (1-4), 285-297.
57. Pan, B.; Pan, B.; Zhang, W.; Lv, L.; Zhang, Q.; Zheng, S., Development of polymeric and polymer-based hybrid adsorbents for pollutants removal from waters. *Chem. Eng. J.* **2009**, *151*, 19-29.
58. Hong, C.; Zhang, W.; Pan, B.; Lv, L.; Han, Y.; Zhang, Q., Adsorption and desorption hysteresis of 4-nitrophenol on a hyper-cross-linked polymer resin NDA-701. *J. Haz. Materials* **2009**, *168*, 1217-1222.
59. Jiang, J. Q.; Yin, Q.; Zhou, J. L.; Pearce, P., Occurrence and treatment trials of endocrine disrupting chemicals (EDCs) in wastewaters. *Chemosphere* **2005**, *61*, 544-550.

60. Li, P.; Sengupta, A. K., Genesis of selectivity and reversibility for sorption of synthetic aromatic anions onto polymeric sorbents. *Environ. Sci. Technol.* **1998**, *32*, 3756-3766.
61. Pan, B.; Du, W.; Zhang, W.; Zhang, X.; Zhang, Q.; Pan, B.; Lv, L.; Zhang, Q.; Chen, J., Improved adsorption of 4-nitrophenol onto a novel hyper-cross-linked polymer. *Environ. Sci. Technol.* **2007**, *41*, 5057-5962.
62. Pan, B.; Zhang, Q.; Meng, F.; Li, X.; Zhang, X.; Zheng, J.; Zhang, W.; Pan, B.; Chen, J., Sorption enhancement of aromatic sulfonates onto an aminated hyper-cross-linked polymer. *Environ. Sci. Technol.* **2005**, *39*, 3308-3313.
63. Pan, B.; Zhang, W.; Pan, B.; Qiu, H.; Zhang, Q.; Zhang, Q.; Zheng, S., Efficient removal of aromatic sulfonates from wastewater by a recyclable polymer: 2-naphthalene sulfonate as a representative pollutant. *Environ. Sci. Technol.* **2008**, *42*, 7411-7416.
64. Pan, B. P.; Zhang, Q.; Pan, B.; Zhang, W.; Du, W.; Ren, H., Removal of aromatic sulfonates from aqueous media by aminated polymeric sorbents: Concentration-dependent selectivity and the application. *Micropor. Mesopor. Mat.* **2008**, *116*, 63-69.
65. Streat, M.; Horner, D. J., Adsorption of highly soluble herbicides from water using activated carbon and hypercrosslinked polymers. *Trans IChemE* **2000**, *78*, 363-382.
66. Xu, Z.; Zhang, Q.; Fang, H. H. P., Application of porous resin sorbents in industrial wastewater treatment and resource recovery. *Crit. Rev. Env. Sci. Tec.* **2003**, *33*, 363-389.
67. Pan, B.; Pan, B.; Zhanga, W.; Lv, L.; Zhang, Q.; Zheng, S., Development of polymeric and polymer-based hybrid adsorbents for pollutants removal from waters. *Chem Eng J* **2009**, *151*, (13), 19-29.

68. Pan, B.; Zhang, H., A modified Polanyi-based model for mechanistic understanding of adsorption of phenolic compounds onto polymeric adsorbents. *Environ. Sci. Technol.* **2012**, *46*, (12), 6806-6814.
69. Pan, B.; Zhang, H., Interaction mechanisms and predictive model for the sorption of aromatic compounds onto nonionic resins. *J. Phys. Chem. C* **2013**, *117*, 17707–17715.
70. Pan, B.; Zhang, H., Reconstruction of adsorption potential in Polanyi-based models and application to various adsorbents. *Environ. Sci. Technol.* **2014**, *48*, 6772–6779.
71. Abraham, M. H.; Acree Jr, W. E., Equations for the transfer of neutral molecules and ionic species from water to organic phases. *J. Org. Chem.* **2010**, *75*, (4), 1006-1015.
72. Abraham, M. H.; Acree Jr, W. E., Solute descriptors for phenoxide anions and their use to establish correlations of rates of reaction of anions with iodomethane. *J. Org. Chem.* **2010**, *75*, (9), 3021-3026.
73. Bradley, J.-C.; Williams, A.; Lang, A., *Jean-Claude Bradley Open Melting Point Dataset*.
74. Do, D. D., *Adsorption analysis*. World Scientific: 1998.
75. Abraham, M. H.; Ibrahim, A.; Zissimos, A. M., Determination of sets of solute descriptors from chromatographic measurements. *J. Chromatogr. A* **2004**, *1037*, (1), 29-47.
76. Abraham, M. H.; McGowan, J., The use of characteristic volumes to measure cavity terms in reversed phase liquid chromatography. *Chromatographia* **1987**, *23*, (4), 243-246.
77. Abraham, M. H., Scales of solute hydrogen-bonding: their construction and application to physicochemical and biochemical processes. *Chem. Soc. Rev.* **1993**, *22*, (2), 73-83.

78. Zhu, D.; Pignatello, J. J., Characterization of aromatic compound sorptive interactions with black carbon (charcoal) assisted by graphite as a model. *Environ. Sci. Technol.* **2005**, *39*, (7), 2033-2041.
79. Santori, G.; Luberti, M.; Brandani, S., Common tangent plane in mixed-gas adsorption. *Fluid Phase Equilib.* **2015**, *392*, 49-55.
80. Nguyen, T. H.; Cho, H.-H.; Poster, D. L.; Ball, W. P., Evidence for a pore-filling mechanism in the adsorption of aromatic hydrocarbons to a natural wood char. *Environ. Sci. Technol.* **2007**, *41*, (4), 1212-1217.
81. Zhang, W.; Wei, C.; Feng, C.; Ren, Y.; Hu, Y.; Yan, B.; Wu, C., The occurrence and fate of phenolic compounds in a coking wastewater treatment plant. *Water Science & Technology* **2013**, *68*, (2), 433-440.